

Efficient Personalization of Generative Models via Optimal Experimental Design

Guy Schacht¹ Ziyad Sheebaelhamd² Riccardo De Santi^{1,3} Mojmir Mutny^{1,4} Andreas Krause^{1,3}

Abstract

Preference learning from human feedback has the ability to align generative models with the needs of end-users. Human feedback is costly and time-consuming to obtain, which creates demand for data-efficient query selection methods. This work presents a novel approach that leverages optimal experimental design to ask humans the most informative preference queries, from which we can elucidate the latent reward function modeling user preferences efficiently. We formulate the problem of preference query selection as the one that maximizes the information about the underlying latent preference model. We show that this problem has a convex optimization formulation, and introduce a statistically and computationally efficient algorithm ED-PBRL that is supported by theoretical guarantees and can efficiently construct structured queries such as images or text. We empirically present the proposed framework by personalizing a text-to-image generative model to user-specific styles, showing that it requires less preference queries compared to random query selection.

1. Introduction

Generative Models & Reinforcement Learning In recent years, large-scale generative models have demonstrated tremendous success in generating high-fidelity content across various modalities (Brown et al., 2020; Rombach et al., 2022; Brooks et al., 2024). These models produce content through iterative processes: LLMs generate text token by token (Brown et al., 2020; Ouyang et al., 2022) and diffusion models refine outputs over multiple denoising steps (Dhariwal & Nichol, 2021). For this reason, the Reinforcement Learning (RL) paradigm provides a natural framework for controlling and personalizing these models through feedback mechanisms. Several works have successfully leveraged intermediate feedback during generation: LLMs

can be guided through conversational feedback (Ouyang et al., 2022; Christiano et al., 2017), text-to-image models can incorporate human preferences at various generation stages (Lee et al., 2023; Black et al., 2024), and diffusion models can be steered using reward signals during the denoising process (Fan et al., 2023; Clark et al., 2024). This RL framing enables optimizing policies to produce outputs aligned with learned reward functions, improving generation quality (Lee et al., 2023; Xu et al., 2023), ensuring safety constraints (Bai et al., 2022b;a), and personalizing to user preferences (Ouyang et al., 2022; Rafailov et al., 2023; Stiennon et al., 2020).

Preference-Based RL for Personalization Framing the generative process as an RL problem is particularly powerful for personalization, as it allows for aligning the agent’s policy with a user’s subjective taste. The key challenge is that this taste is difficult to formalize as a numerical reward function. Reinforcement Learning from Human Feedback (RLHF) is the established paradigm for this, learning rewards from human-supplied demonstrations or other forms of feedback (Ziebart et al., 2008; Finn et al., 2016; Lindner et al., 2022; Casper et al., 2023). Perhaps the most prominent and practical instance of RLHF is Preference-Based Reinforcement Learning (PBRL), where the latent reward model is learned from comparative feedback (e.g., a user choosing between two generated images). This feedback modality is often more intuitive for humans to provide than absolute scores or full demonstrations (Christiano et al., 2017; Sadigh et al., 2017; Biyik et al., 2020; Ouyang et al., 2022; Saha et al., 2023; Gheshlaghi Azar et al., 2024). After collecting preference feedback from the user, an estimated reward model then serves as the reward signal aligning the RL agent to the human.

PBRL Query Selection via OED The success of PBRL, however, hinges on the accuracy of this learned reward model, which in turn depends on the quality of the preference queries presented for user feedback. Collecting these user preferences is a significant practical bottleneck, as it requires a human to provide numerous labels—a process that is both time-consuming and costly (Ouyang et al., 2022; Lee et al., 2023). This data collection bottleneck makes sample efficiency paramount, which requires selecting maximally informative queries. Existing PBRL methods for selecting such queries often face a trade-off: they are either computa-

¹ETH Zurich, Zurich, Switzerland ²Max Planck Institute for Intelligent Systems, Tübingen, Germany ³ETH AI Center, Zurich, Switzerland ⁴Broad Institute, Boston, USA. Correspondence to: Guy Schacht <guysc1993@gmail.com>.

tionally tractable but lack theoretical guarantees, or they are theoretically grounded but computationally expensive (Saha et al., 2023; Wu & Sun, 2024; Sadigh et al., 2017; Zhan et al., 2023; Saha et al., 2023). This raises a fundamental question for making personalization practical:

Can we find policies that select queries for preference-based feedback in a way that is both statistically efficient, and computationally tractable?

In this work, we address this question by leveraging the principles of Optimal Experimental Design (OED) (Chaloner & Verdinelli, 1995; Pukelsheim, 2006; Fedorov & Hackl, 1997). We propose a method to select the most informative queries to present to the user, ensuring that the preference model is learned with as few interactions as possible. Specifically, our objective is to determine a set of K distinct exploration policies for the agent that generate queries. These policies are carefully chosen to generate informative set of queries. When the user provides feedback on these, they provide maximal information about their latent reward parameters. We achieve this by reformulating the generally intractable OED problem (Pukelsheim, 2006; Fedorov & Hackl, 1997) into a continuous optimization problem over the space of state visitation measures induced by the exploration policies. This allows us to use Convex Reinforcement Learning (Hazan et al., 2019) to efficiently compute the optimal set of policies for query generation. In tabular settings, we prove that our objective is concave and global optimal solution can be reached.

Our contributions We provide the following:

- We formalize the problem of query selection for generative models with Markov processes (Sec. 3), and propose ED-PBRL, a method that builds on Optimal Experimental Design to efficiently solve the problem of learning preferences from a minimal number of queries in the Markov process (Sec. 4). Our method advances the intersection between RLHF theory and practice, by being theoretically principled and at the same time applicable to real-life settings.
- A novel upper bound on the MSE matrix of the (regularized) MLE in terms of the (regularized) Fisher information matrix, obtained via a self-concordant analysis (App. B.1).
- Assuming a generative model on discrete space, we provide global convergence guarantees for ED-PBRL based on Convex-RL (Sec. 5.1).
- An experimental evaluation of the proposed method on three types of experiments: synthetic ground truth models, LLM-simulated preference feedback (using GPT-

4.1-mini as a human proxy), and also REINFORCE-based optimization applying a stochastic version of our objective to GPT2 based exploration policies. Our method showcases promising performance for the personalization of text-to-image models (Sec. 6).

We further show that our framework extends beyond fixed vocabularies: in Appendix C, we present a vocabulary-free variant that optimizes LLM prompt generators directly via REINFORCE (Williams, 1992), avoiding the need for pre-computed embedding matrices.

2. Related Work

Generative Model Guidance Generative models, especially diffusion models (Ho et al., 2020; Sohl-Dickstein et al., 2015; Dhariwal & Nichol, 2021) and Large Language Models (LLMs), have achieved remarkable success, and often benefit from guidance to align outputs with user preferences. For diffusion models, guidance techniques steer pre-trained models by incorporating preference information, for example, through gradients from an auxiliary classifier (*classifier guidance* (Dhariwal & Nichol, 2021; Song et al., 2021)) or by leveraging conditional model properties (*classifier-free guidance* (Ho & Salimans, 2022)). Similarly, LLMs are often guided in a post-training phase to better align with user intent; for instance, InstructGPT (Ouyang et al., 2022) uses human feedback to fine-tune models to follow instructions. The effectiveness of these methods often hinges on an accurate underlying preference model. Our work focuses on efficiently learning such preference models to enhance personalized generative model guidance.

Preference-Based Reinforcement Learning A key challenge in realizing effective generative model guidance is the accurate and efficient learning of the underlying user preference models. Preference-Based Reinforcement Learning (PBRL) offers a powerful paradigm for this, learning rewards (and thus preference models) from comparative feedback, which is often more intuitive for humans than providing explicit reward values or detailed demonstrations. PBRL’s focus on preferences aligns well with capturing nuanced user tastes for guidance. Many PBRL advancements focus on statistical efficiency and regret guarantees (Chen et al., 2022; Saha et al., 2023; Zhan et al., 2023; Saha et al., 2023). However, these methods can rely on computationally expensive components, such as oracles for selecting informative queries over pairs of policies from an exponentially large set, or complex algorithmic structures (Wu & Sun, 2024). Our work differs by focusing on a computationally tractable method for query selection in PBRL. We optimize a set of K exploration policies to generate informative comparative queries using an experiment design (ED) objective, rather than relying on pairwise policy comparison oracles. Closest to our goal are two related methods. Information

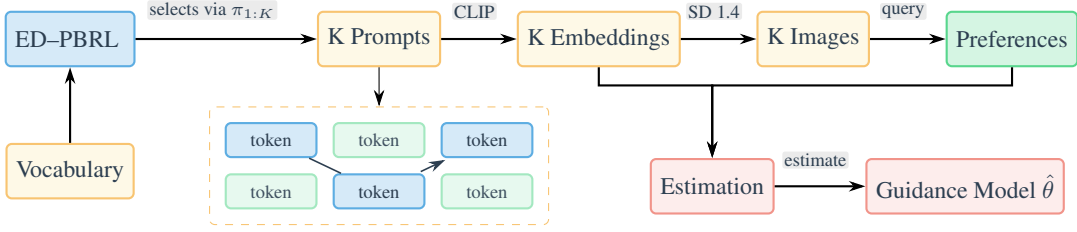


Figure 1. The personalization workflow: ED-PBRL calculates policies π_1, \dots, π_K which select prompts in the combinatorial token space. These prompts are embedded (CLIP) and rendered with Stable Diffusion 1.4 (Rombach et al., 2022); preferences on the resulting images are collected and used to estimate the guidance model $\hat{\theta}$. Each prompt is formed by a sequence of tokens—a trajectory of a policy π_i . The K policies are chosen so that, for a given budget, the preferences and embeddings yield an accurate estimate of the guidance model. Notice that each policy can be parameterized via a large table or as a separate generative language model.

Directed Reward Learning (IDRL) (Lindner et al., 2021) selects queries to disambiguate return differences between a maintained set of plausibly optimal policies; maintaining such a candidate set can be restrictive in large spaces. Schlaginhaufen et al. (2025) et. al apply OED to perform offline query selection, but they solve a sequential OED problem by repeatedly selecting from a precomputed trajectory space which is exponentially large. They rely on submodularity of the D-optimal criteria and therefore limited to it. They offer regret guarantees, but those carry a $\sqrt{\kappa}$ factor, typically exponential in the reward parameter norm. By contrast, we reformulate the design problem over *state visitation measures*, which reduces the search space from exponential (trajectories) to polynomial (occupancy measures), supports any concave matrix-monotone scalarization (A-, V-, D-optimal), and yields a globally optimal solution via convex optimization.

Optimal Experiment Design To efficiently learn preference models for guidance, the queries presented to the user must be highly informative. Optimal Experimental Design (OED) (Pukelsheim, 2006; Fedorov & Hackl, 1997) provides principles for selecting experiments to maximize information gain, often by optimizing scalar criteria of the Fisher Information Matrix. Due to the NP-hardness of discrete design, continuous relaxations optimizing over design measures are common. Mutny et al. (2023); Wagenmaker & Jamieson (2022) and Folch et al. (2024) applied OED to active exploration in Markov Chains by optimizing over visitation measures of a single policy. Our work adapts OED to PBRL by designing a *set of K policies* for generating informative *comparative queries*, whilst making it tractable using the framework of convex Reinforcement Learning (Convex-RL) (Hazan et al., 2019; Zahavy et al., 2021).

3. Problem Setting

We frame the task of personalized content generation as an RL problem, where the agent sequentially appends to or refines its output. The reward function is unknown and

defines the latent personal user’s taste. The agent’s goal is to learn this latent reward model using the fewest preference queries possible to be given user feedback upon.

3.1. Markov Decision Process

To formalize the control of generative models, we employ a finite-horizon Markov Decision Process (MDP) defined by the tuple $\mathcal{M} = (\mathcal{S}, \mathcal{A}, P, H)$. Here, \mathcal{S} and \mathcal{A} represent the state and action spaces, $P(s'|s, a)$ is the *known* transition matrix governing the dynamics of the generation process, and H is the finite horizon. A policy $\pi(a|s)$ defines the agent’s strategy for making sequential choices.

Examples of MDPs for Generative Models Our abstract MDP formulation is intentionally general. To make this concrete, we provide several examples of how it can be instantiated:

Automatic Prompt Engineering: The sequential construction of prompts for text-to-image models can be modeled as an MDP, where states are timesteps in prompt construction and actions are choices of design tokens (full words or phrases) from a fixed vocabulary. This is the formulation used in our main experiments (Section 6).

Autoregressive Text Generation: For an LLM, a state is the sequence of tokens generated so far, and an action is selecting the next token (BPE subword) from the model’s vocabulary. We demonstrate this formulation in Appendix C, where policies are parameterized as GPT-2 models optimized via REINFORCE.

Iterative Refinement in Diffusion Models: A state can be the noisy data (e.g., an image) at a denoising step, and an action could be selecting a guidance direction for refinement.

3.2. Latent Reward and Preference Feedback

We model the user’s latent reward as linear in known features: a map $\phi : \mathcal{S} \times \mathcal{A} \rightarrow \mathbb{R}^d$ embeds state-action pairs, and $r(s, a) = (\theta^*)^\top \phi(s, a)$ for an unknown $\theta^* \in \mathbb{R}^d$. The goal is to estimate θ^* with $\hat{\theta}$ efficiently from preferences. The framework and guarantees extend to richer classes (e.g., RKHS linear functionals, c.f. (Mutny et al., 2023)). For clarity the reward is only state dependent, e.g. $r(s) = (\theta^*)^\top \phi(s)$. This is without loss of generality as state-action rewards are recovered by augmenting state space as $\mathcal{S}' = \mathcal{S} \times \mathcal{A}$.

Preference model To learn θ^* , we rely on comparative feedback. Given K options (e.g. states, actions or trajectories), denoted by $\{x_1, \dots, x_K\}$, a user selects the one they prefer most. We model the probability of this choice using the standard multinomial logit (softmax) model. The probability that a user chooses option x_q is then:

$$P(x_q \text{ is best}) = \frac{\exp((\theta^*)^\top \phi(x_q))}{\sum_{k'=1}^K \exp((\theta^*)^\top \phi(x_{k'}))} \quad (1)$$

where $\phi(x'_k)$ is the feature vector of option x'_k . This model is a generalization of the Bradley-Terry model (which corresponds to $K = 2$) (Bradley & Terry, 1952).

3.3. Interaction Protocol

The learning process follows a fixed experimental design protocol with three phases:

- 1. Policy Optimization:** The algorithm determines a set of K exploration policies, π_1, \dots, π_K , by solving an information-maximization optimization problem (detailed in Section 4).
- 2. Data Collection:** The K policies are executed for T episodes, generating T sets of trajectories. Each set is $\{\tau_{t,1}, \dots, \tau_{t,K}\}$, where $\tau_{t,q} \sim \pi_q$. These sets (or their components, see below) are presented to the user, who provides one preference choice at each of the H timesteps, resulting in a dataset of $T \times H$ feedback comparisons.
- 3. Parameter Estimation:** Using the collected feedback and the features of the corresponding trajectories, the algorithm computes the final estimate $\hat{\theta}$ of the true parameter θ^* .

The central challenge, which we address, is how to perform Phase 1 to select policies that make the estimation in Phase 3 as efficient as possible. The pipeline is visualized in Figure 1 with image feedback generated via prompts (trajectories).

3.4. Feedback Models

We consider two plausible models for how feedback is elicited over the generated trajectories.

State-based Preference Feedback At each timestep $h \in [H]$, the user compares states $\{s_{1,h}, \dots, s_{K,h}\}$ from the K trajectories. The choice probability is given by Eq. 1 using state features $\phi(s_{q,h})$. This model is mainly used for our theoretical analysis.

Truncated Trajectory Preference Feedback More practically, the user compares partial outputs. The options x_q are trajectories truncated at step h , which we denote as a sequence of states $\tau_q[1 : h] = \{s_{q,1}, \dots, s_{q,h}\}$. For example, in prompt generation, users compare partial prompts like “A painting of...” vs. “A photo of...”. The choice probability is again given by Eq. 1, but using features of the partial sequence, $\phi(\tau_q[1 : h])$. These features (e.g., a CLIP embedding of a partial sentence) are not necessarily simple sums of their constituent state features. We use this model in our experiments.

3.5. Estimation

Given a dataset of $T \times H$ preferences, the parameter θ^* is estimated via regularized maximum likelihood. Let $y_{t,h,q}$ be a one-hot indicator that alternative q was chosen at step h of episode t . The probability of this choice, $p(q|t, h, \theta)$, is given by the softmax model from Eq. 1 applied to the features of the options presented under the relevant feedback model. The estimate $\hat{\theta}$ is the solution to $\hat{\theta} =$

$$\arg \max_{\theta \in \mathbb{R}^d} \sum_{t=1, h=1, q=1}^{T, H, K} y_{t,h,q} \log(p(q|t, h, \theta)) - \frac{\lambda}{2} \|\theta\|_2^2 \quad (2)$$

where $\lambda \geq 0$ is a regularization coefficient.

4. Optimal Experimental Design for Preference Learning

Our main motivation is to select queries for PBRL in a sample efficient manner. *Given a budget T , how should we select K exploration policies to generate T sets of K trajectories that are maximally informative for estimating θ^* ?* To address this, we use an information-theoretic approach, leveraging the Fisher Information Matrix.

4.1. Fisher Information and Estimation Error

The quality of the estimate $\hat{\theta}$ is fundamentally linked to which queries are selected. The Fisher Information Matrix (FIM), $I(\theta)$, quantifies the information content of the data; classically, the Cramér–Rao Lower Bound (CRLB) relates $I(\theta)$ to a *lower* bound on the covariance of unbiased estimators. In our setting, we establish a *novel upper bound* for the regularized MLE—derived via a self-concordant analysis of the (regularized) log-likelihood: the Mean Squared Error (MSE) matrix of θ_λ is controlled by the inverse of the regularized FIM at the true parameter, $I_\lambda(\theta^*)^{-1}$. This is formalized in the following result.

Theorem 4.1 (Maximizing FIM improves Estimation). *Un-*

der mild conditions (Appendix B.1), the expected square error of $\hat{\theta}_\lambda$, of multinomial likelihood, satisfies

$$\mathbb{E}[(\hat{\theta}_\lambda - \theta^*)(\hat{\theta}_\lambda - \theta^*)^T] \preceq C_{\theta^*}^\lambda \cdot I_\lambda(\theta^*)^{-1}$$

where $C_{\theta^*}^\lambda = (1 - r_{\theta^*}^\lambda)^{-4}$ depends on a local consistency radius $r_{\theta^*}^\lambda \in [0, 1)$.

Thus, maximizing $I_\lambda(\theta^*)$ (making its inverse smaller in Loewner order) reduces estimation error; see Appendix B.1 for the full proof.

4.2. The Intractable Ideal Objective

Theorem 4.1 motivates maximizing the FIM $I_\lambda(\theta^*)$ to minimize estimation error. Our goal is therefore to select policies that generate trajectories yielding the most information. However, optimizing the FIM over a discrete set of $K \times T$ trajectories is typically NP-hard. A standard OED approach is to relax this problem by optimizing over a *distribution* of experiments—in our case, policies that generate trajectories. This leads to optimizing the *expected* FIM that the policies induce (Pukelsheim, 2006; Fedorov & Hackl, 1997).

The expected regularized FIM for K policies $\pi_{1:K}$ generating T episodes is:

$$I_\lambda(\pi_{1:K}, \theta) = T \sum_{h=1}^H I_h(\pi_{1:K}, \theta) + \lambda I_d, \quad (3)$$

where $I_h(\pi_{1:K}, \theta)$ is the FIM contribution from timestep h , averaged over the trajectory distributions η_{π_q} . Let s_h^q be the state of trajectory $\tau_q \sim \eta_{\pi_q}$ at step h . The expression for I_h is an expectation over the FIM for a single multinomial choice (derived in Appendix B.2):

$$I_h(\pi_{1:K}, \theta) = \mathbb{E}_{\substack{\tau_q \sim \eta_{\pi_q} \\ q \in [K]}} \left[\sum_{q=1}^K p(q|h) \phi(s_h^q) \phi(s_h^q)^\top - \left(\sum_{q=1}^K p(q|h) \phi(s_h^q) \right) \left(\sum_{l=1}^K p(l|h) \phi(s_h^l) \right)^\top \right] \quad (4)$$

where $p(q|h)$ is the softmax choice probability for the states $\{s_h^1, \dots, s_h^K\}$, as defined in (1). The ideal policy then optimizes the objective:

$$\arg \max_{\pi_{1:K}} s(I_\lambda(\pi_{1:K}, \theta)) \quad (5)$$

However, this ideal objective presents two major challenges:

- **Dependence on unknown θ :** The FIM depends on the true θ , which is unknown at the design stage.
- **Intractable Optimization:** The objective involves an expectation over an exponentially large trajectory space ($\mathcal{S} \times \mathcal{S} \times \dots \times \mathcal{S}$, H times) of K independent policies.

4.3. Reformulation to a Tractable Objective

We address these issues by deriving a tractable objective in three steps; full details appear in App. B.4.

Step 1: Reformulation using State Visitation Measures.

We rewrite the expected FIM in terms of state visitation measures (occupancy measures), turning policy expectations into expectations over $s \sim d_{\pi_q}^h$. This yields a design objective over visitation measures; see Lemma B.2. Appendix Sec. B.4 gives the explicit form and the Step 1 problem statement.

Step 2: θ -agnostic approximation. The per-step information depends on the unknown θ through the choice probabilities $p(\cdot)$. Appendix Sec. B.4 gives the explicit expression. To decouple design from θ without assuming the worst case θ , we adopt an average-case approach and replace $p(q|h; s_{1:K}, \theta)$ by its expectation under an uninformative prior, giving $p(q|h; s_{1:K}) \approx 1/K$. For $K=2$ this holds exactly with a Gaussian prior on θ ; for $K>2$ it is a reasonable approximation when alternatives are diverse/symmetric. Substituting yields a θ -independent surrogate $\tilde{I}_h(d_{1:K}^h)$; see Appendix Eq. 12.

Step 3: Marginalization The expectation in the approximate FIM (Eq. 12) can be resolved into a tractable matrix form. It decomposes into per-timestep contributions $\tilde{I}_h(d_{1:K}^h)$ as:

$$\tilde{I}_h(d_{1:K}^h) = \Phi^T \left(\frac{1}{K} \sum_{q=1}^K \text{diag}(d_q^h) - \bar{d}^h (\bar{d}^h)^T \right) \Phi, \quad (6)$$

where Φ is the matrix of concatenated state features, d_q^h is the visitation vector for policy q at step h , and $\bar{d}^h = \frac{1}{K} \sum_q d_q^h$ is the average visitation. We show this formally in Theorem B.3. The approximated information matrix in Eq. (6) depends on $|S| \times H \times K$ variables for discrete state spaces and can be efficiently optimized upon proper scalarization.

Scalarization The objective (6) is a matrix-valued function of $d_{1:K}$. As such, it cannot be directly optimized, since the information about different components θ_i of the latent reward needs to be weighted. Classically, experiment design (Fedorov & Hackl, 1997) suggests weighting all components of uncertainty equally such as reducing $\|\hat{\theta} - \theta^*\|^2$, or minimizing error on a certain projection $(\hat{\theta} - \theta^*)^\top \mathbf{V}(\hat{\theta} - \theta^*)$. These are called A- or V-designs, respectively, and result in a particular scalarization function $s(\cdot)$. With scalarization our final design objective is:

$$\begin{aligned} \arg \max_{d_{1:K} \in \mathcal{D}} s(I_{\text{total}}(d_{1:K})) &:= \\ \arg \max_{d_{1:K} \in \mathcal{D}} s \left(T \sum_{h=1}^H \tilde{I}_h(d_{1:K}^h) + \lambda I_d \right) \end{aligned} \quad (7)$$

For A-design this is $s(\mathbf{A}) = 1/\text{Tr}(\mathbf{A}^{-1})$, and for V-design, $s(\mathbf{A}) = 1/\text{Tr}(\mathbf{V}\mathbf{A}^{-1})$. This optimization is subject to the constraints that each d_q^h must be a valid visitation of policy π_q (i.e. $\in \mathcal{D}$).

4.4. Information Relationship of Feedback Models

The objective (Eq. 7) is derived for the state-based feedback model. Arguably, the more practical variant is the truncated trajectory feedback model. In the following result, we provide a link between state-based and truncated-trajecotry-based feedback using additive feature decomposition assumption, and prove that by optimizing a policy for state-based feedback design in Eq. 7 we also improve the truncated-trajecotry design with the same policy.

Theorem 4.2 (Truncated trajectory). *If the features of the partial trajectory admit additive decomposition, i.e. $\phi(\tau[1:h]) = \sum_j^h \phi(s_j)$, the approximate Fisher Information (FI) of truncated trajectory feedback is lower-bounded by the FI of the state-based feedback scaled by 1/4.*

This result is formally stated and proven as Theorem B.5 in Appendix B.5.

5. The ED-PBRL Algorithm and Guarantees

In this section, we summarize the optimization and the interaction protocol. In particular, we present a *static* version of ED-PBRL algorithm. We first determine K policies by maximizing the objective in Eq. 7. Here $d_{1:K} = \{d_q^h\}_{q \in [K], h \in [H]}$ are (state) visitation measures of the K policies. These then generate trajectories (e.g. prompts) for preference collection, after which we fit $\hat{\theta}$. See Alg. 1.

Algorithm 1 ED-PBRL (Conceptual Overview)

Input: MDP details (M, Φ) , design parameters $(K, H, T, s(\cdot), \lambda)$

Output: Estimated preference parameter $\hat{\theta}$

Phase 1: Compute Optimal State Visitation Measures

Solve Eq. 7 for optimal visitation measures $\{d_q^{*h}\}_{h,q}$.

Phase 2: Policy Extraction and Trajectory Sampling

Extract policies $\{\pi_q^*\}_{q=1}^K$ from $\{d_q^{*h}\}_{h,q}$.

Sample $K \times T$ trajectories using $\{\pi_q^*\}$ and collect preference feedback.

Phase 3: Parameter Estimation

Estimate $\hat{\theta}$ using all collected feedback (cf. Section 3).

The solver in *Phase 1* uses the Frank–Wolfe algorithm, which sequentially linearizes the objective and solve the linearized problem over the visitation measures. Let $x \in \mathcal{S}$ denote a state, and let $d_{1:K}$ collect the visitation measures for all policies. The algorithm update the policies in iterative fashion, at iterate n , for each policy q define the per-policy linearization of Eq.(7) $G_q^{(n)}(x) := \nabla_{d_q(x)} s(I_{\text{total}}(d_{1:K}^{(n)}))$, evaluated at the current iterate $d_{1:K}^{(n)}$. The linearization decouples across policies and can be solved separately. For

a single policy $q \in [K]$, denote by d_{π_q} its visitation vector. The linearization oracle for this policy solves:

$$\Delta d_{\pi_q}^{n+1} = \arg \max_{d \in \mathcal{D}} \sum_{x \in \mathcal{S}} d(x) G_q^{(n)}(x)$$

where \mathcal{D} is the convex set of valid visitation measures, and \sum turns to \int for continuous state spaces. The linear oracle problem exactly coincides with the reinforcement learning problem where $G_q^{(n)}(x)$ plays the role of reward, a key observation from the Convex-RL (Hazan et al., 2019; Zahavy et al., 2021). The next iterate is constructed using convex combination $d_{\pi_q}^{(n+1)} = \alpha_{n+1} d_{\pi_q}^{(n)} + (1 - \alpha_{n+1}) \Delta d_{\pi_q}^{n+1}$ chosen via line search oracle. After sufficient number of steps, we extract policies π via marginalization $\pi_q^*(a | s) \propto d_{\pi_q}^*(s, a)$. Afterwards in *Phase 2* and *3*, we sample $K \times T$ trajectories and estimate $\hat{\theta}$. See Appendix Alg. 2 for more detailed description.

5.1. Theoretical Guarantees and Algorithm Variants

Frank–Wolfe (FW) is known to provably converge to maximum on concave objectives defined on convex sets for well chosen sequence of α_n . The set of visitation measures is convex as it is a polytope, and we show the objective is concave.

Theorem 5.1. *Let $d_{1:K} = \{d_q^h\}_{h \in [H], q \in [K]}$. If the scalarization $s : \mathbb{S}_+^d \rightarrow \mathbb{R}$ is concave and matrix-monotone, then $(I_{\text{total}}(d_{1:K}))$ as defined in (7) is concave in $d_{1:K}$.*

FW converges to the global optimum with the standard $\mathcal{O}(1/n)$ rate under an exact linear oracle (Jaggi, 2013). Detailed statements and proofs (including the oracle instantiation and concavity proof) are provided in Appendix Sec. B.7.

Adaptive variant The *static* version does not use partial feedback from prior queries to update policies π_q $q \in [K]$. We can run, an *adaptive* variant where collect a batch of preferences, update $\hat{\theta}$, then re-optimize visitation and hence policies π_q . Round 1 uses $p \approx 1/K$, but with adaptive variant we could use an estimated $\hat{p}(q | h)$ (e.g. via $\hat{\theta}$) inside the objective and refine intermediate visitation measures.

6. Experimental Evaluation

We evaluate our framework to personalize text-to-image generation based on CLIP embeddings (Radford et al., 2021). We conduct two types of experiments: (1) a quantitative evaluation using synthetic ground truth (GT) models to simulate user preferences, and (2) an LLM-simulated preference study using GPT-4.1-mini as a human proxy. We also validate a vocabulary-free extension using REINFORCE in Appendix C. The experimental workflow is shown in Figure 1.

Experimental Methodology We briefly comment on the overall setup; full details are in Appendix Sec. A. We construct a prompt in a finite-horizon MDP; states are timesteps

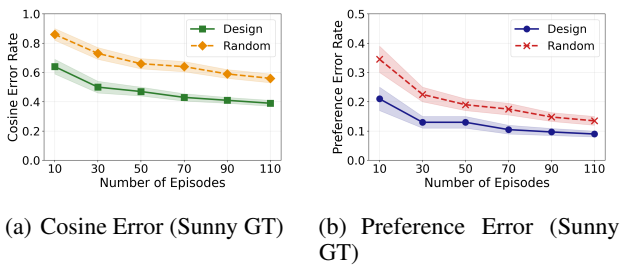


Figure 2. Performance of ED-PBRL on the Sunny synthetic Ground Truth (GT) model. We plot the Cosine Error (left) and Preference Prediction Error (right) against the number of interaction episodes. These results demonstrate the efficiency of our OED approach. Numerical results for all GT models (Sunny, Medieval, and Technological) are presented in Appendix (Figure 6).

($H = 6$), actions are design tokens from a fixed vocabulary, and a trajectory yields a prompt. We randomly select an initial *base-prompt*, which represents the overall content of the image. Token and prompt features are embedded using CLIP, and preferences are modeled linearly via the Truncated Trajectory Feedback model (see Sec. 3.4). Design is optimized with the V-design scalarization (Sec. 4.3) where the matrix V contains concatenated prompt embeddings of base prompts (see App. A.1 for details). A consolidated list of hyperparameters appears in Table 2 (Appendix A).

6.1. Synthetic Ground Truth Model Experiments

We perform quantitative evaluation of ED-PBRL against known ground truth (GT) preference models. We simulate a user whose preferences are dictated by a GT linear preference model θ^* . Each GT model is constructed from the normalized CLIP text embedding of a descriptive sentence. For instance, the *Sunny GT* model, which is the focus of our main results, uses the phrase “*An image with warm colors depicting bright sunshine*”. We also evaluate against *Medieval* and *Technological GT* models, with full details provided in Appendix A.2. The goal is to measure how accurately and efficiently our method recovers θ^* . We report two metrics (Appendix A.2): **Cosine Error**—the cosine distance between the learned preference vector $\hat{\theta}$ and the GT vector θ^* ; and **Preference Prediction Error**—the error rate of $\hat{\theta}$ in predicting the synthetic user’s preference on unseen pairs of prompts from a held-out test token set.

Figure 2 presents the learning curves for these metrics for the *Sunny GT* model, averaged over multiple independent runs. Similar trends hold across the remaining models (see Appendix Figure 6).

6.2. LLM-Simulated Preference Experiment

To systematically evaluate our approach across many experimental conditions, we use an LLM (GPT-4.1-mini) as a simulated preference oracle. The LLM receives the same

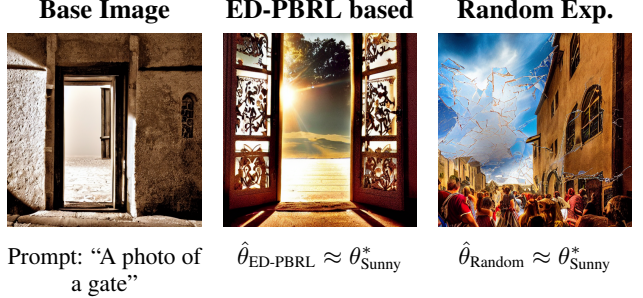


Figure 3. Sunny GT qualitative personalization. ED-PBRL queries yield better preference estimates than random exploration. The ED-PBRL image better matches the “sunny” aesthetic.

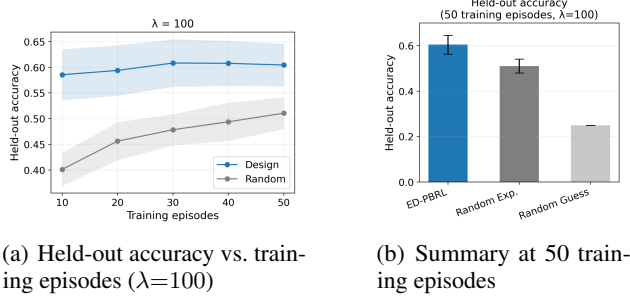
questionnaire-style queries that would be shown to human participants: four candidate images and a style description, with the task of selecting the image that best matches the specified style. This enables comprehensive evaluation across multiple regularization strengths, training set sizes, and aesthetic styles—a scale prohibitively expensive with human participants.

Setup We evaluate ten target style conditions spanning diverse aesthetics: futuristic, sunny, forest, landscape, ancient, noir, watercolor, cyberpunk, minimalist, and medieval. For each style, the LLM receives a descriptive prompt (e.g., “Futuristic style with advanced technologies”) and selects among $K=4$ candidate images at each step $h \in \{1, \dots, H\}$ (with $H=6$). We systematically vary regularization $\lambda \in \{0.1, 1, 10, 100\}$ and training episodes $\in \{10, 20, 30, 40, 50\}$, with 10 held-out test episodes. Each configuration is repeated across 3 cross-validation folds.

Evaluation Metric We evaluate models by how well the learned $\hat{\theta}$ predicts held-out LLM choices. The held-out benchmark consists of 10 episodes ($10 \times H=60$ decisions). We report the held-out preference accuracy: the fraction of test decisions where the predicted best trajectory matches the LLM’s choice. Results are averaged across styles and folds. Figure 4(a) shows accuracy vs. training episodes at $\lambda=100$, while Figure 4(b) summarizes accuracy at 50 episodes.

6.3. Vocabulary-Free REINFORCE Extension

The previous approach was limited by a finite vocabulary defining the state-space. This is, however, not necessary for our setup. In the following, we show how to optimize LLM prompt generators directly via the Policy Gradient style algorithm, specifically REINFORCE (Williams, 1992), by using policy parameterization. This allows us to formulate a vocabulary-free extension where K policies are implemented using separate LLMs (MagicPrompt fine-tuned GPT2’s) to generate prompts directly, removing the need for a fixed token set. For each policy (LLM) q , we denote all its



(a) Held-out accuracy vs. training episodes ($\lambda=100$)

(b) Summary at 50 training episodes

Figure 4. LLM-simulated held-out preference accuracy. (a) shows accuracy vs. training episodes at $\lambda=100$ (shaded: s.e. over 10 styles). (b) summarizes accuracy at 50 episodes. ED-PBRL stays near $\sim 60\%$; random exploration degrades with less data. Random-guess baseline is $1/K=25\%$.

Table 1. Comparison of Frank–Wolfe and REINFORCE.

	Frank–Wolfe	REINFORCE
Prompt space	Fixed vocabulary \mathcal{S}	Unrestricted
Exploration policy	$d_q \in \Delta^{ \mathcal{S} }$	LLM p_{θ_q}
FIM optimality	Eq. 7	Eq. 22 (App. C)
Optimization	Convex	Non-convex
Iteration (gradient) complexity	$\mathcal{O}(K H \mathcal{S})$	$\mathcal{O}(H T M K)$

trainable parameters as θ_q , then a prompt $\tau_q = (w_1, \dots, w_H)$ yields CLIP prefix embeddings $\phi(\tau_q[1:H])$. For a single trajectory of K prompts, the per-position Fisher contribution:

$$I_h = \frac{1}{K} \sum_{q=1}^K \phi_q^{(h)} (\phi_q^{(h)})^\top - \mu_h \mu_h^\top, \mu_h = \frac{1}{K} \sum_{q=1}^K \phi_q^{(h)}$$

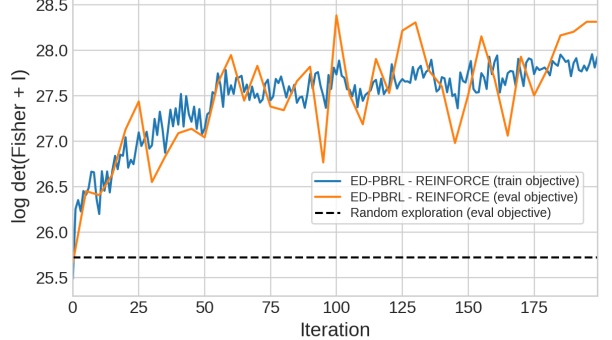
We aggregate T trajectories and maximize the D-optimal objective $I = \sum_{t=1}^T \sum_{h=1}^H I_h^{(t)} + \lambda I_d$, where $\mathcal{L} = \log \det(I)$. Optimization uses REINFORCE (Williams, 1992) with a batch-mean baseline: for meta-samples $m = 1, \dots, M$,

$$\nabla_{\theta_q} \mathbb{E}[\mathcal{L}] \approx \frac{1}{M} \sum_{m=1}^M (\mathcal{L}_m - \bar{\mathcal{L}}) \nabla_{\theta_q} \log p_{\theta_q}(\mathcal{T}_q^{(m)}), \quad (8)$$

where $\mathcal{T}_q^{(m)}$ collects the T prompts from policy q in meta-sample m , \mathcal{L}_m are the M objectives of the batch, and $\bar{\mathcal{L}}$ their average. This uses only on-the-fly CLIP embeddings and scales to unrestricted vocabularies. Full details are in Appendix C. The key differences between the REINFORCE approach and the Frank-Wolfe approach presented earlier are summarized in Table 1. Notice that when $|\mathcal{S}| \gg T \cdot M$ parametrization of policy with an LLM is also more computationally efficient. For our experiments $T \times M = 64$, while $|\mathcal{S}| > 1000$.

7. Conclusion

We introduced ED-PBRL, a principled optimization framework with global convergence guarantees for efficiently



(a) Optimization trajectory

Random policies

Optimized policies

(b) t-SNE of CLIP embeddings

Figure 5. REINFORCE experimental validation. (a) D-optimal objective $\log \det(I)$ over $N=200$ policy gradient iterations. Training (blue) and evaluation (orange, every 5 iterations) curves stay aligned, confirming stable optimization. The gray dotted line shows the objective value of the random (unoptimized) MagicPrompt GPT-2 baseline, which remains flat as its policy is never updated. (b) t-SNE of CLIP embeddings (100 prompts per policy): left shows the random baseline, right shows ED-PBRL (REINFORCE). The optimized policies form $K = 4$ distinct CLIP clusters, demonstrating that our exploration strategy produces diverse yet structured queries.

personalizing generative models by learning user preferences from a minimal number of comparative queries. Our work provides a theoretical analysis and justification for the practice of Reinforcement-Learning from Human Feedback (RLHF). Our experiments use specific models (CLIP, MagicPrompt fine-tuned GPT-2, Stable Diffusion 1.4) to demonstrate that the principles of Optimal Experimental Design (OED) are effectively applied to real-life generative models. These underlying models can be freely substituted with any advanced generative model, as long as they possess a Markov structure. ED-PBRL accelerates the learning of latent reward functions for each user, opening an avenue to personalize generative AI tools *through optimization*, with fewer interactions compared to random query selection. Our experiments show that the framework scales beyond fixed vocabulary settings to unrestricted language generation by parameterizing policies as LLMs using policy gradient techniques with the same information measuring quantities.

Impact Statement

This paper studies ML algorithm that influences data collection. Such algorithms may generate long-term biases in collected datasets and need to be used cautiously. Since these algorithms construct queries with which real users interact, there needs to be a comprehensive framework including ethics standards to ensure they are not causing harm to humans. There are many potential consequences of our work if we use it in products to personalize generative models. Our study is only a proof-of-concept visualizing formalism to perform such personalization. The aspect of bias needs to be further investigated before any deployment, which was out of the scope of this work.

Ethics Statement. This paper uses LLM-simulated preferences (GPT-4.1-mini) rather than human participants for the preference learning experiments. This approach avoids ethical concerns related to human subject research while enabling systematic evaluation across many experimental conditions. The LLM receives the same questionnaire-style queries that would be shown to human participants, making the evaluation protocol directly transferable to human studies in future work.

References

Bai, Y., Jones, A., Ndousse, K., Askell, A., Chen, A., Das-Sarma, N., Drain, D., Fort, S., Ganguli, D., Henighan, T., et al. Training a helpful and harmless assistant with reinforcement learning from human feedback. *arXiv preprint arXiv:2204.05862*, 2022a. URL <https://arxiv.org/abs/2204.05862>.

Bai, Y., Kadavath, S., Kundu, S., Askell, A., Kernion, J., Jones, A., Chen, A., Goldie, A., Mirhoseini, A., McKinnon, C., et al. Constitutional ai: Harmlessness from ai feedback. *arXiv preprint arXiv:2212.08073*, 2022b. URL <https://arxiv.org/abs/2212.08073>.

Biyik, E., Palan, M., Landolfi, N. C., Losey, D. P., and Sadigh, D. Asking easy questions: A user-friendly approach to active reward learning. In Kaelbling, L. P., Kräig, D., and Sugiura, K. (eds.), *Proceedings of the Conference on Robot Learning*, volume 100 of *Proceedings of Machine Learning Research*, pp. 1177–1190. PMLR, 30 Oct–01 Nov 2020. URL <https://proceedings.mlr.press/v100/biyik20a.html>.

Black, K., Janner, M., Du, Y., Kostrikov, I., and Levine, S. Training diffusion models with reinforcement learning. In *The Twelfth International Conference on Learning Representations*, 2024. URL <https://openreview.net/forum?id=YCWjhGrJFD>.

Bradley, R. A. and Terry, M. E. Rank analysis of incomplete block designs: I. the method of paired comparisons. *Biometrika*, 39(3/4):324–345, 1952. ISSN 00063444, 14643510. URL <http://www.jstor.org/stable/2334029>.

Brooks, T., Peebles, B., Holmes, C., DePue, W., Guo, Y., Jing, L., Schnurr, D., Taylor, J., Luhman, T., Luhman, E., et al. Video generation models as world simulators. *OpenAI Blog*, 1(8):1, 2024.

Brown, T., Mann, B., Ryder, N., Subbiah, M., Kaplan, J. D., Dhariwal, P., Neelakantan, A., Shyam, P., Sastry, G., Askell, A., Agarwal, S., Herbert-Voss, A., Krueger, G., Henighan, T., Child, R., Ramesh, A., Ziegler, D., Wu, J., Winter, C., Hesse, C., Chen, M., Sigler, E., Litwin, M., Gray, S., Chess, B., Clark, J., Berner, C., McCandlish, S., Radford, A., Sutskever, I., and Amodei, D. Language Models are Few-Shot Learners. In Larochelle, H., Ranzato, M., Hadsell, R., Balcan, M., and Lin, H. (eds.), *Advances in Neural Information Processing Systems*, volume 33, pp. 1877–1901. Curran Associates, Inc., 2020. URL https://proceedings.neurips.cc/paper_files/paper/2020/file/1457c0d6bfc4967418bfb8ac142f64a-Paper.pdf.

Casper, S., Davies, X., Shi, C., Gilbert, T. K., Scheurer, J., Rando, J., Freedman, R., Korbak, T., Lindner, D., Freire, P., et al. Open problems and fundamental limitations of reinforcement learning from human feedback. *arXiv preprint arXiv:2307.15217*, 2023. URL <https://arxiv.org/abs/2307.15217>.

Chaloner, K. and Verdinelli, I. Bayesian experimental design: A review. *Statistical science*, pp. 273–304, 1995.

Chen, X., Zhong, H., Yang, Z., Wang, Z., and Wang, L. Human-in-the-loop: Provably efficient preference-based reinforcement learning with general function approximation. In Chaudhuri, K., Jegelka, S., Song, L., Szepesvari, C., Niu, G., and Sabato, S. (eds.), *Proceedings of the 39th International Conference on Machine Learning*, volume 162 of *Proceedings of Machine Learning Research*, pp. 3773–3793. PMLR, 17–23 Jul 2022. URL <https://proceedings.mlr.press/v162/chen22ag.html>.

Christiano, P. F., Leike, J., Brown, T., Martic, M., Legg, S., and Amodei, D. Deep reinforcement learning from human preferences. *Advances in neural information processing systems*, 30, 2017.

Clark, K., Vicol, P., Swersky, K., and Fleet, D. J. Directly fine-tuning diffusion models on differentiable rewards. In *The Twelfth International Conference on Learning Representations*, 2024. URL <https://openreview.net/forum?id=YCWjhGrJFD>.

Representations, 2024. URL <https://openreview.net/forum?id=1vmSEVL19f>.

Dhariwal, P. and Nichol, A. Diffusion models beat gans on image synthesis. *Advances in neural information processing systems*, 34:8780–8794, 2021.

Fan, Y., Watkins, O., Du, Y., Liu, H., Ryu, M., Boutilier, C., Abbeel, P., Ghavamzadeh, M., Lee, K., and Lee, K. Dpok: Reinforcement learning for fine-tuning text-to-image diffusion models. *Advances in Neural Information Processing Systems*, 36:79858–79885, 2023.

Fedorov, V. V. and Hackl, P. *Model-oriented design of experiments*, volume 125. Springer, 1997.

Finn, C., Levine, S., and Abbeel, P. Guided cost learning: Deep inverse reinforcement learning via policy optimization. In *International conference on machine learning*, pp. 49–58. PMLR, 2016. URL <https://proceedings.mlr.press/v48/finn16.html>.

Folch, J. P., Tsay, C., Lee, R., Shafei, B., Ormaniec, W., Krause, A., van der Wilk, M., Misener, R., and Mutny, M. Transition constrained bayesian optimization via markov decision processes. *Advances in Neural Information Processing Systems*, 37:88194–88235, 2024.

Frank, M. and Wolfe, P. An algorithm for quadratic programming. *Naval research logistics quarterly*, 3(1-2): 95–110, 1956.

Gheshlaghi Azar, M., Daniel Guo, Z., Piot, B., Munos, R., Rowland, M., Valko, M., and Calandriello, D. A general theoretical paradigm to understand learning from human preferences. In Dasgupta, S., Mandt, S., and Li, Y. (eds.), *Proceedings of The 27th International Conference on Artificial Intelligence and Statistics*, volume 238 of *Proceedings of Machine Learning Research*, pp. 4447–4455. PMLR, 02–04 May 2024. URL <https://proceedings.mlr.press/v238/gheshlaghi-azar24a.html>.

Hazan, E., Kakade, S., Singh, K., and Van Soest, A. Provably efficient maximum entropy exploration. In *International Conference on Machine Learning*, pp. 2681–2691. PMLR, 2019. URL <https://proceedings.mlr.press/v97/hazan19a/hazan19a.pdf>.

Ho, J. and Salimans, T. Classifier-free diffusion guidance, 2022. URL <https://arxiv.org/abs/2207.12598>.

Ho, J., Jain, A., and Abbeel, P. Denoising diffusion probabilistic models. *Advances in neural information processing systems*, 33:6840–6851, 2020.

Jaggi, M. Revisiting Frank-Wolfe: Projection-free sparse convex optimization. In Dasgupta, S. and McAllester, D. (eds.), *Proceedings of the 30th International Conference on Machine Learning*, volume 28 of *Proceedings of Machine Learning Research*, pp. 427–435, Atlanta, Georgia, USA, 17–19 Jun 2013. PMLR. URL <https://proceedings.mlr.press/v28/jaggi13.html>.

Lee, K., Liu, H., Ryu, M., Watkins, O., Du, Y., Boutilier, C., Abbeel, P., Ghavamzadeh, M., and Gu, S. S. Aligning text-to-image models using human feedback, 2023. URL <https://arxiv.org/abs/2302.12192>.

Lindner, D., Turchetta, M., Tschiatschek, S., Ciosek, K., and Krause, A. Information directed reward learning for reinforcement learning. In Ranzato, M., Beygelzimer, A., Dauphin, Y., Liang, P., and Vaughan, J. W. (eds.), *Advances in Neural Information Processing Systems*, volume 34, pp. 3850–3862. Curran Associates, Inc., 2021. URL https://proceedings.neurips.cc/paper_files/paper/2021/file/1fa6269f58898f0e809575c9a48747ef-Paper.pdf.

Lindner, D., Krause, A., and Ramponi, G. Active exploration for inverse reinforcement learning. *Advances in Neural Information Processing Systems*, 35:5843–5853, 2022.

Mutný, M. *Modern Adaptive Experiment Design: Machine Learning Perspective*. PhD thesis, ETH Zurich, 2024.

Mutný, M., Janik, T., and Krause, A. Active exploration via experiment design in markov chains. In Ruiz, F., Dy, J., and van de Meent, J.-W. (eds.), *Proceedings of The 26th International Conference on Artificial Intelligence and Statistics*, volume 206 of *Proceedings of Machine Learning Research*, pp. 7349–7374. PMLR, 25–27 Apr 2023. URL <https://proceedings.mlr.press/v206/mutny23a.html>.

Ouyang, L., Wu, J., Jiang, X., Almeida, D., Wainwright, C., Mishkin, P., Zhang, C., Agarwal, S., Slama, K., Ray, A., et al. Training language models to follow instructions with human feedback. *Advances in neural information processing systems*, 35:27730–27744, 2022.

Pukelsheim, F. *Optimal Design of Experiments*. Society for Industrial and Applied Mathematics, 2006. doi: 10.1137/1.9780898719109. URL <https://pubs.siam.org/doi/abs/10.1137/1.9780898719109>.

Puterman, M. L. *Markov Decision Processes: Discrete Stochastic Dynamic Programming*. John Wiley & Sons, 2014.

Radford, A., Kim, J. W., Hallacy, C., Ramesh, A., Goh, G., Agarwal, S., Sastry, G., Askell, A., Mishkin, P., Clark, J., et al. Learning transferable visual models from natural language supervision. In *International conference on machine learning*, pp. 8748–8763. PMLR, 2021.

Rafailov, R., Sharma, A., Mitchell, E., Manning, C. D., Ermon, S., and Finn, C. Direct preference optimization: Your language model is secretly a reward model. *Advances in neural information processing systems*, 36: 53728–53741, 2023.

Rombach, R., Blattmann, A., Lorenz, D., Esser, P., and Ommer, B. High-resolution image synthesis with latent diffusion models. In *Proceedings of the IEEE/CVF conference on computer vision and pattern recognition*, pp. 10684–10695, 2022.

Sadigh, D., Dragan, A., Sastry, S., and Seshia, S. Active preference-based learning of reward functions. *UC Berkeley*, 2017. doi: <https://doi.org/10.15607/rss.2017.xiii.053>. URL <https://escholarship.org/uc/item/88k894w7>.

Saha, A., Pacchiano, A., and Lee, J. Dueling rl: Reinforcement learning with trajectory preferences. In *International conference on artificial intelligence and statistics*, pp. 6263–6289. PMLR, 2023.

Schlaginhaufen, A., Ouhamma, R., and Kamgarpour, M. Efficient preference-based reinforcement learning: Randomized exploration meets experimental design. In *The Thirty-ninth Annual Conference on Neural Information Processing Systems*, 2025. URL <https://openreview.net/forum?id=qEfgajdKea>.

Sohl-Dickstein, J., Weiss, E., Maheswaranathan, N., and Ganguli, S. Deep unsupervised learning using nonequilibrium thermodynamics. In Bach, F. and Blei, D. (eds.), *Proceedings of the 32nd International Conference on Machine Learning*, volume 37 of *Proceedings of Machine Learning Research*, pp. 2256–2265, Lille, France, 07–09 Jul 2015. PMLR. URL <https://proceedings.mlr.press/v37/sohl-dickstein15.html>.

Song, Y., Sohl-Dickstein, J., Kingma, D. P., Kumar, A., Ermon, S., and Poole, B. Score-based generative modeling through stochastic differential equations. In *International Conference on Learning Representations*, 2021. URL <https://openreview.net/forum?id=PxtIG12RRHS>.

Stiennon, N., Ouyang, L., Wu, J., Ziegler, D., Lowe, R., Voss, C., Radford, A., Amodei, D., and Christiano, P. F. Learning to summarize with human feedback. *Advances in neural information processing systems*, 33:3008–3021, 2020.

Wagenmaker, A. and Jamieson, K. G. Instance-dependent near-optimal policy identification in linear mdps via online experiment design. *Advances in Neural Information Processing Systems*, 35:5968–5981, 2022.

Williams, R. J. Simple statistical gradient-following algorithms for connectionist reinforcement learning. *Machine learning*, 8(3):229–256, 1992.

Wu, R. and Sun, W. Making RL with preference-based feedback efficient via randomization. In *The Twelfth International Conference on Learning Representations*, 2024. URL <https://openreview.net/forum?id=Pe2lo3QOvo>.

Xu, J., Liu, X., Wu, Y., Tong, Y., Li, Q., Ding, M., Tang, J., and Dong, Y. Imagereward: Learning and evaluating human preferences for text-to-image generation. *Advances in Neural Information Processing Systems*, 36: 15903–15935, 2023.

Zahavy, T., O’Donoghue, B., Desjardins, G., and Singh, S. Reward is enough for convex mdps. *Advances in Neural Information Processing Systems*, 34:25746–25759, 2021.

Zhan, W., Uehara, M., Kallus, N., Lee, J. D., and Sun, W. Provable offline reinforcement learning with human feedback. In *ICML 2023 Workshop The Many Facets of Preference-Based Learning*, 2023.

Ziebart, B. D., Maas, A. L., Bagnell, J. A., and Dey, A. K. Maximum entropy inverse reinforcement learning. In *Aaai*, volume 8, pp. 1433–1438, 2008.

Table 2. Summary of experimental parameters.

Common Parameters (All Experiments)			
Num. Policies (K)	4	CLIP Model	ViT-L/14
Feedback Model	Truncated Trajectory		
Synthetic Experiment		LLM-Simulated Preference Experiment	
Horizon (H)	6	Horizon (H)	6
OED Criterion	V-design (App. A.1)	OED Criterion	V-design (App. A.1)
Frank-Wolfe Iters	100	Frank-Wolfe Iters	100
Feedback Source	GT Model	Feedback Source	GPT-4.1-mini
Num. Episodes (T)	10, 30, ..., 110	Num. Episodes (T)	60
Num. Runs	25	Episode Split	Benchmark 10
Num. Test Prompts	1000	Cross-Validation	3 folds
Num. Eval Pairs	5000	Regularization (λ)	100
Vocabulary Split	75% train / 25% test	Num. Styles	10
Regularization (λ)	100	Evaluation Metrics	App. A.3
Evaluation Metrics	App. A.2		
Vocabulary-Free REINFORCE (App. C)			
Base LLM	MagicPrompt (GPT-2)	Horizon (H)	8 words
Trajectories (T)	8	MC Samples (M)	8
Regularization (λ)	1	Objective	D-opt (log det)
Optimizer	SGD	Learning Rate (η)	10^{-3}
Baseline	Batch-mean	Iterations	200

A. Appendix: Detailed Experimental Setup

This section provides a comprehensive description of the experimental environment, parameters, and models used in our evaluation, intended for reproducibility and completeness. The overall workflow is depicted in Figure 1. A summary of key parameters is available in Table 2.

A.1. Common Experimental Components

Environment: Prompt Construction MDP The environment is modeled as a finite-horizon Markov Decision Process (MDP) designed to simulate the construction of textual prompts.

- **States (\mathcal{S}):** States $s \in \{0, 1, \dots, H - 1\}$ directly correspond to the current timestep or depth in the prompt construction process.
- **Horizon (H):** The horizon corresponds to the number of vocabulary files used for sequential token selection.
- **Actions (\mathcal{A}):** Actions are indices corresponding to unique "design tokens" extracted from the vocabulary files. These tokens represent semantic concepts (e.g., "Man sitting", "artistic", "happy").
- **Vocabulary:** The vocabulary is sourced from H files: 'bases.txt', 'ambient.txt', 'style.txt', 'composition.txt', 'lighting.txt', 'detail.txt'. The selection of tokens is structured by timestep. At $s = 0$, only "base" concepts are allowed. For $s > 0$, tokens from other categories are used.
- **Transitions (P):** Deterministic. Selecting a token at state s transitions to state $s + 1$.
- **Feature Representation for OED ($\phi(a)$):** The features for design tokens are their 768-dimensional, normalized CLIP text embeddings ('ViT-L/14').

Preference Model and Estimation

- **Feedback Model:** We use the Truncated Trajectory Feedback model (Section 3.4) for both experiments. At each timestep h , a preference is given over K partial prompts $\{\tau_1[0 : h], \dots, \tau_K[0 : h]\}$.

- **Features for Estimation ($\phi(\text{partial prompt})$):** The feature vector for a partial prompt is its normalized CLIP text embedding ('ViT-L/14').

Experimental Design (OED) The experimental design objective is to select policies that maximize information about θ .

- **Scalarization Criterion $s(\cdot)$:** We use an A-optimality variant, $s(I_{total,reg}) = -\text{Tr}(V(I_{total,reg})^{-1})$, where $I_{total,reg}$ is the regularized total approximate FIM from Eq. 7.
- **V Matrix Construction:** The matrix $V = C^T C$ is constructed from differences between feature embeddings of tokens from the same thematic category (excluding 'bases.txt'), i.e., $c_k^T = (\phi(a_i) - \phi(a_j))^T$. This V-design criterion directly targets the precision of estimated preference differences, which is essential for learning an effective ranking model. The full construction is detailed in the original appendix text.
- **Optimization:** The Convex-RL procedure (Algorithm 2) is used to solve the design problem.
- **Computational Cost:** The one-time design optimization for a vocabulary of approximately 5000 tokens takes around 10 minutes on a single NVIDIA A100 GPU.

A.2. Synthetic Ground Truth Model Experiments: Setup and Metrics

Ground Truth Scorer Models For the synthetic experiments, we simulate user preferences using three distinct ground truth (GT) scorer models. Each is represented by a weight vector $\theta^* \in \mathbb{R}^d$ constructed by taking the normalized CLIP text embedding of a descriptive sentence:

- **Sunny GT Model (θ_{sunny}^*):** From CLIP ("An image with warm colors depicting bright sunshine").
- **Medieval GT Model ($\theta_{medieval}^*$):** From CLIP ("An image with ancient kingdom depicting medieval times").
- **Technological GT Model ($\theta_{technological}^*$):** From CLIP ("An image with advanced technologies depicting futuristic style").

The GT vector θ^* is used to simulate user choices and serves as the ground truth for evaluation.

Evaluation Metrics

- **Cosine Error:** $1 - \text{cosine_similarity}(\hat{\theta}, \theta^*)$. Measures the angular deviation between the estimated preference vector and the ground truth θ^* .
- **Preference Prediction Error:** The fraction of pairs where $\hat{\theta}$'s prediction mismatches the GT's preference on prompts generated exclusively from the held-out testing vocabulary.

A.3. LLM-Simulated Preference Experiment: Setup and Metrics

Setup To enable systematic evaluation across many experimental conditions, we use GPT-4.1-mini as a simulated preference oracle. The LLM receives the identical questionnaire-style queries that would be shown to human participants: at each decision point, it sees four candidate images and a style description, and must select the image that best matches the specified style. This approach enables comprehensive evaluation across multiple regularization strengths ($\lambda \in \{0.1, 1, 10, 100\}$), training set sizes ($\{10, 20, 30, 40, 50\}$ episodes), and ten aesthetic styles—a scale that would be prohibitively expensive with human participants.

LLM Query Format The LLM receives the following prompt structure for each preference query:

```
You are an art reviewer.  
Follow the style guidance below
```

and choose the single best preference label.
 Return only a strict JSON object
 in the format {"preference": "<label>"}.
 Do not include explanations or additional fields.

Style guidance:
 [STYLE DESCRIPTION]

The style description (e.g., “Futuristic style with advanced technologies”) is substituted for each of the ten target styles. The four candidate images are presented, and the LLM returns its preference.

Cross-Validation Protocol For robust evaluation, we use 3-fold cross-validation with rotating test windows. With 60 total episodes per style-algorithm pair, each fold uses 50 episodes for training and 10 for testing. The test window rotates across folds: fold 0 tests on episodes 50–59, fold 1 on episodes 40–49, and fold 2 on episodes 30–39.

Evaluation Metric

- **Hold-out Preference Accuracy:** We measure how well the learned model predicts the LLM’s choices on unseen data. This is the percentage of times that the preference predicted by $\hat{\theta}$ (i.e., $\arg \max_q \hat{\theta}^\top \phi(\tau_q[1:h])$) matches the actual choice made by the LLM on the 10 held-out test episodes. With a horizon of $H = 6$, this evaluation is performed over $10 \times 6 = 60$ preference decisions per fold, aggregated across 3 folds and 10 styles.

A.4. Full Numerical and Qualitative Results

This section provides the full set of results for all experiments.

Synthetic Experiment Results

Qualitative Results Summary (Synthetic) For each Ground Truth (GT) model (Sunny, Medieval, Technological), Figures 7, 8, and 9 show a visual comparison of the prompts generated by ED-PBRL (Design) and Random exploration. The figures correspond to the median cosine error run (out of 25 seeds) after $T = 110$ feedback episodes with $K = 4$ policies. To test generalization, the personalized prompts are constructed by adding style tokens selected from the held-out test vocabulary to a base prompt.

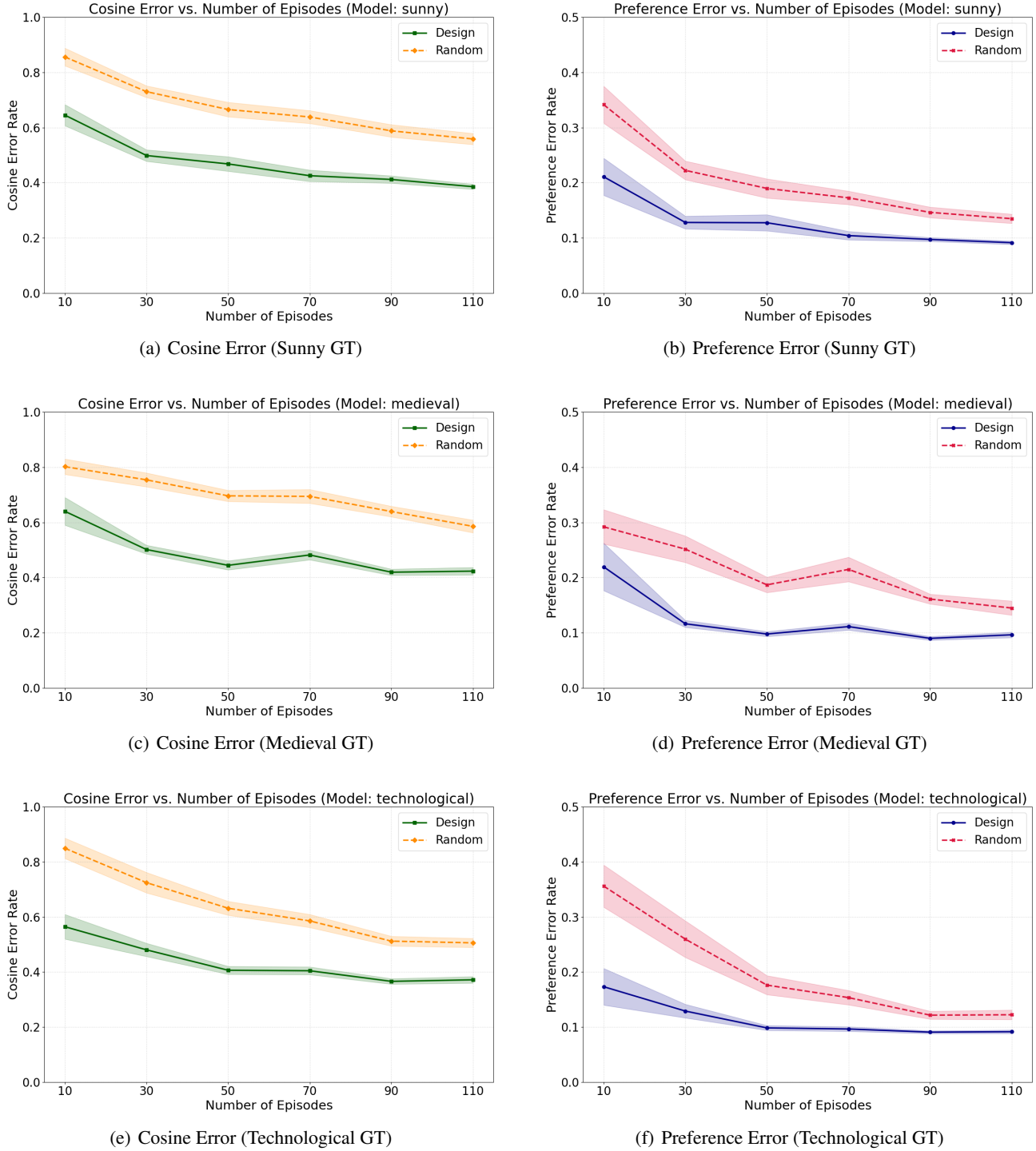
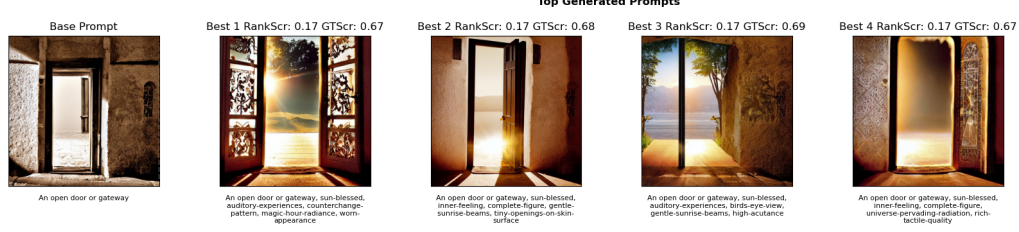


Figure 6. Performance of ED-PBRL on Sunny, Medieval, and Technological synthetic Ground Truth (GT) models. For each GT model, we plot the Cosine Error (left column) and Preference Prediction Error (right column) against the number of interaction episodes. Results are averaged over $N=25$ independent runs, and the shaded regions represent the standard error of the mean. The Sunny GT model results are also shown in the main paper (Figure 2).



(a) ED-PBRL (Design) - Top Prompts for Sunny GT



(b) Random Exploration - Top Prompts for Sunny GT

Figure 7. Full summary of top generated prompts for the Sunny GT Model. The images compare prompts generated via ED-PBRL (Design) and Random exploration. Each personalized image is annotated with its estimated score from the learned model (RankScore) and its true score from the ground truth model (GTScore), where a higher GTScore indicates better alignment with the target 'Sunny' aesthetic. Note that ED-PBRL consistently finds prompts that yield higher GT Scores, demonstrating its superior personalization capability.



(a) ED-PBRL (Design) - Top Prompts for Medieval GT

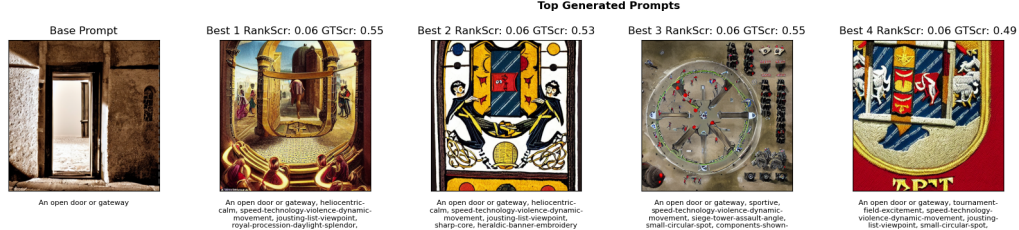


(b) Random Exploration - Top Prompts for Medieval GT

Figure 8. Full summary of top generated prompts for the Medieval GT Model. The images compare prompts generated via ED-PBRL (Design) and Random exploration. Each personalized image is annotated with its estimated score from the learned model (RankScore) and its true score from the ground truth model (GTScore), where a higher GTScore indicates better alignment with the target 'Medieval' aesthetic. Note that ED-PBRL consistently finds prompts that yield higher GT Scores, demonstrating its superior personalization capability.



(a) ED-PBRL (Design) - Top Prompts for Technological GT



(b) Random Exploration - Top Prompts for Technological GT

Figure 9. Full summary of top generated prompts for the Technological GT Model. The images compare prompts generated via ED-PBRL (Design) and Random exploration. Each personalized image is annotated with its estimated score from the learned model (RankScore) and its true score from the ground truth model (GTScore), where a higher GTScore indicates better alignment with the target 'Technological' aesthetic. Note that ED-PBRL consistently finds prompts that yield higher GT Scores, demonstrating its superior personalization capability.

Qualitative Results from Preliminary Human Study To illustrate how learned preference models generalize to new prompts, we present qualitative results from a preliminary human study. A participant whose stated preference was for “forestry images with a lot of green, nature and landscapes” provided feedback during the exploration phase. After training, we tested the learned models ($\hat{\theta}_{\text{ED-PBRL}}$ and $\hat{\theta}_{\text{Random}}$) on four new base prompts chosen by the participant. The following figures show the top-ranked personalized images generated by each model.



(a) ED-PBRL (Design) - Top Prompts for "Reflecting last year"



(b) Random Exploration - Top Prompts for "Reflecting last year"

Figure 10. Top generated prompts for the base prompt “Reflecting last year” from the preliminary human study. Images are ranked by the score from the respective learned models (RankScore).



(a) ED-PBRL (Design) - Top Prompts for "A novice boxer"

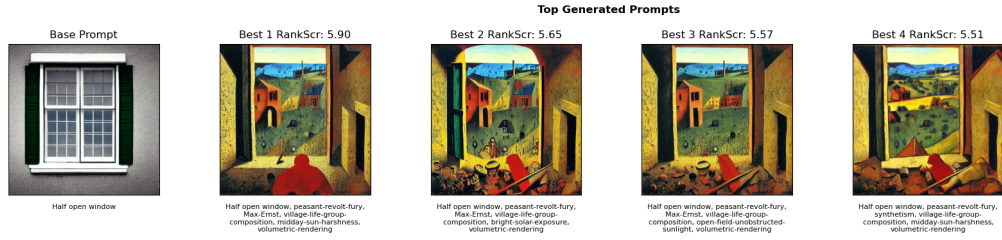


(b) Random Exploration - Top Prompts for "A novice boxer"

Figure 11. Top generated prompts for the base prompt “A novice boxer” from the preliminary human study.



(a) ED-PBRL (Design) - Top Prompts for "Half open window"

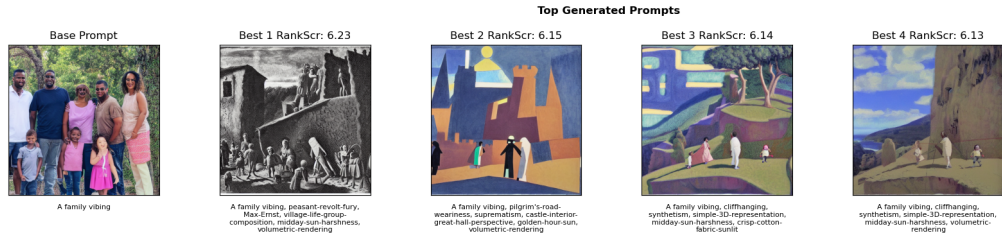


(b) Random Exploration - Top Prompts for "Half open window"

Figure 12. Top generated prompts for the base prompt “Half open window” from the preliminary human study.



(a) ED-PBRL (Design) - Top Prompts for "A family vibing"



(b) Random Exploration - Top Prompts for "A family vibing"

Figure 13. Top generated prompts for the base prompt “A family vibing” from the preliminary human study.

Per-Style Panels (All Ten Styles) Figure 14 shows per-style held-out accuracy curves for all ten styles (futuristic, sunny, forest, landscape, ancient, noir, watercolor, cyberpunk, minimalist, medieval) at $\lambda = 100$. Each subplot reports mean held-out accuracy across 3 cross-validation folds for ED-PBRL and Random; curves are shown at training sizes 10/20/30/40/50 episodes with 10 episodes held out for testing.

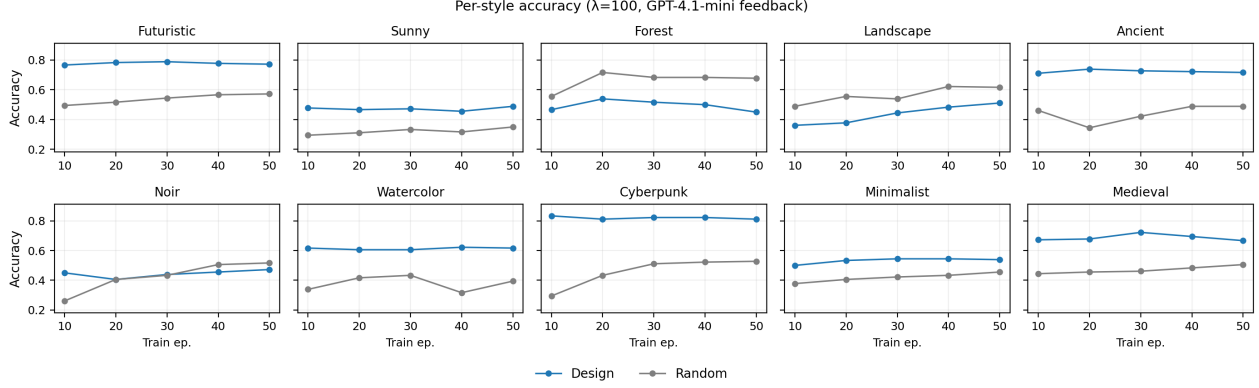


Figure 14. LLM-simulated preference study, all ten styles, $\lambda = 100$: per-style held-out accuracy (10 test episodes). ED-PBRL consistently outperforms random exploration across most styles, with the advantage being most pronounced when training data is limited.

Comprehensive Results Table Table 3 lists per-style held-out accuracies at $\lambda = 100$ for both ED-PBRL (Design) and Random exploration, their differences in percentage points, and the number of hold-out comparisons. Results are shown for 50 training episodes with 10 held-out test episodes, averaged across 3 cross-validation folds.

Table 3. LLM-simulated preference held-out accuracy by style at $\lambda = 100$ and 50 training episodes. Accuracy values are in percentage points; Diff is Design minus Random. Hold-out consists of 10 test episodes (60 comparisons), averaged across 3 cross-validation folds.

Style	Design (%)	Random (%)	Diff (pp)
Futuristic	77.2	57.2	+20.0
Sunny	48.9	35.0	+13.9
Forest	45.0	67.8	-22.8
Landscape	51.1	61.7	-10.6
Ancient	71.7	48.9	+22.8
Noir	47.2	51.7	-4.4
Watercolor	61.7	39.4	+22.2
Cyberpunk	81.1	52.8	+28.3
Minimalist	53.9	45.6	+8.3
Medieval	66.7	50.6	+16.1
Average	60.4	51.1	+9.4

B. Appendix: Proofs, Derivations and Further Results

B.1. Relationship between Estimation Error and Fisher Information

We formalize the link between estimation error and information used in the main text. For the regularized MLE θ_λ , we show that the Mean Squared Error (MSE) matrix is controlled by the inverse of the regularized Fisher Information at the true parameter θ^* :

$$\mathbb{E}[(\theta_\lambda - \theta^*)(\theta_\lambda - \theta^*)^\top] \preceq C_{\theta^*}^\lambda \cdot I_\lambda(\theta^*)^{-1}.$$

The proof relies on a self-concordant analysis of the (regularized) log-likelihood to relate the random Hessian to $I_\lambda(\theta^*)$ within a local neighborhood of θ^* . We state the precise assumptions next and then provide the full proof.

B.1.1. ASSUMPTIONS FOR THE MSE BOUND

The derivation of the bound relies on two key assumptions. We state them formally here before proceeding with the proof.

Assumption B.1 (Uniform Local Consistency). *For a given experimental design (policies, T , λ), we assume the regularized MLE θ_λ is close to the true parameter θ^* . Specifically, we assume there exists a constant $r_{\theta^*}^\lambda \in [0, 1)$, dependent on the problem parameters but not on the random data realization, that uniformly bounds the distance between θ_λ and θ^* in the local norm defined by the FIM at θ^* :*

$$\|\theta_\lambda - \theta^*\|_{I(\theta^*)} \equiv \sqrt{(\theta_\lambda - \theta^*)^\top I(\theta^*) (\theta_\lambda - \theta^*)} \leq r_{\theta^*}^\lambda$$

This assumption is a prerequisite for our finite-sample analysis. It allows us to define a data-independent constant $C_{\theta^}^\lambda = (1 - r_{\theta^*}^\lambda)^{-4}$ that can be moved outside the expectation in the proof, simplifying the analysis. Standard large-sample theory for MLE suggests that for a sufficiently large number of samples, this condition is expected to hold with high probability.*

Assumption B.2 (Bounded True Parameter). *The squared ℓ_2 -norm of the true parameter vector θ^* is bounded relative to the regularization strength λ :*

$$\|\theta^*\|_2^2 \leq \frac{1}{\lambda}$$

This assumption, which is standard in the analysis of ridge regression and regularized estimators (Mutný, 2024), constrains the magnitude of the true parameter relative to the regularization strength. It ensures that the bias introduced by the ℓ_2 penalty does not overwhelm the information-related terms in the analysis. In matrix terms, this implies $\lambda^2 \theta^ (\theta^*)^\top \preceq \lambda I_d$.*

With these conditions explicitly stated, we can now present the formal theorem and its proof.

Theorem B.1 (Upper Bound on MSE). *Let θ_λ be the regularized maximum likelihood estimator and θ^* be the true parameter. Under Assumptions B.1 and B.2, the Mean Squared Error (MSE) matrix of the estimator is bounded by:*

$$\mathbb{E}[(\theta_\lambda - \theta^*)(\theta_\lambda - \theta^*)^\top] \preceq C_{\theta^*}^\lambda \cdot I_\lambda(\theta^*)^{-1}$$

where $I_\lambda(\theta^) = I(\theta^*) + \lambda I_d$ is the regularized Fisher Information Matrix at the true parameter, and $C_{\theta^*}^\lambda = (1 - r_{\theta^*}^\lambda)^{-4}$ is a constant determined by the radius $r_{\theta^*}^\lambda$ from Assumption B.1.*

Proof. The proof proceeds in three main steps. First, we establish an exact expression for the estimation error using a Taylor expansion. Second, we use the self-concordance property of the negative log-likelihood, combined with Assumption B.1, to bound the random Hessian that appears in the error expression. Finally, we combine these results and use Assumption B.2 to derive the upper bound on the MSE.

Step 1: Taylor Expansion of the Score Function. The estimator θ_λ is the solution to the regularized maximum likelihood problem, defined by the first-order optimality condition $s_\lambda(\theta_\lambda) = 0$. The regularized score function $s_\lambda(\theta)$ is the gradient of the regularized log-likelihood:

$$\begin{aligned} s_\lambda(\theta) &= \nabla L_{reg}(\theta) \\ &= \sum_{t=1}^T \sum_{q=1}^K (y_{t,q} - p_{t,q}(\theta)) x_{t,q} - \lambda \theta \end{aligned}$$

The Hessian of the negative regularized log-likelihood is the regularized Fisher Information Matrix:

$$I_\lambda(\theta) = -\nabla^2 L_{reg}(\theta) = I(\theta) + \lambda I_d.$$

Note that $\nabla s_\lambda(\theta) = -I_\lambda(\theta)$.

By the vector-valued Mean Value Theorem (a form of Taylor's theorem), we can expand the function $s_\lambda(\theta)$ around the true parameter θ^* :

$$\begin{aligned} 0 &= s_\lambda(\theta_\lambda) \\ &= s_\lambda(\theta^*) + \nabla s_\lambda(\theta_\tau)(\theta_\lambda - \theta^*) \end{aligned}$$

for some θ_τ on the line segment between θ^* and θ_λ . Substituting $\nabla s_\lambda(\theta_\tau) = -I_\lambda(\theta_\tau)$, we get:

$$0 = s_\lambda(\theta^*) - I_\lambda(\theta_\tau)(\theta_\lambda - \theta^*)$$

Rearranging gives the exact expression for the estimation error:

$$\theta_\lambda - \theta^* = I_\lambda(\theta_\tau)^{-1} s_\lambda(\theta^*)$$

The MSE matrix is therefore given by the expectation:

$$\mathbb{E}[(\theta_\lambda - \theta^*)(\theta_\lambda - \theta^*)^T] = \mathbb{E} \left[I_\lambda(\theta_\tau)^{-1} s_\lambda(\theta^*) \times s_\lambda(\theta^*)^\top I_\lambda(\theta_\tau)^{-1} \right]$$

Step 2: Bounding the Hessian via Self-Concordance. The main difficulty is relating the terms $I_\lambda(\theta_\tau)$ and $s_\lambda(\theta^*)$ in the error expression, as they are evaluated at different points. We resolve this by bounding the Hessian term $I_\lambda(\theta_\tau)$ using the self-concordance property of the unregularized negative log-likelihood function, $L(\theta) = -\log P(\text{data}|\theta)$.

The negative log-likelihood for multinomial logistic regression is a sum of log-sum-exp functions, which is a standard example of a self-concordant function. Its Hessian is the Fisher Information Matrix, $I(\theta) = \nabla^2 L(\theta)$. For a self-concordant function f , the Hessians at two points x, y are related by

$$(1 - \|y - x\|_x)^2 \nabla^2 f(x) \preceq \nabla^2 f(y)$$

provided that the local norm $\|y - x\|_x = \sqrt{(y - x)^T \nabla^2 f(x) (y - x)}$ is less than 1.

We now invoke Assumption B.1. It states that $\|\theta_\lambda - \theta^*\|_{I(\theta^*)} \leq r_{\theta^*}^\lambda < 1$ for all data realizations. Since θ_τ lies on the line segment between θ^* and θ_λ , it is necessarily closer to θ^* in any norm, including the local norm defined by $I(\theta^*)$. Thus,

$$\|\theta_\tau - \theta^*\|_{I(\theta^*)} \leq \|\theta_\lambda - \theta^*\|_{I(\theta^*)} \leq r_{\theta^*}^\lambda.$$

Applying the self-concordance property with $f(\theta) = L(\theta)$, $x = \theta^*$, and $y = \theta_\tau$, we get a lower bound on the unregularized FIM:

$$I(\theta_\tau) \succeq (1 - \|\theta_\tau - \theta^*\|_{I(\theta^*)})^2 I(\theta^*) \succeq (1 - r_{\theta^*}^\lambda)^2 I(\theta^*)$$

This inequality holds deterministically for any realization of the data due to our assumption. We use this to bound the regularized FIM:

$$\begin{aligned}
 I_\lambda(\theta_\tau) &= I(\theta_\tau) + \lambda I_d \\
 &\succeq (1 - r_{\theta^*}^\lambda)^2 I(\theta^*) + \lambda I_d \\
 &\succeq (1 - r_{\theta^*}^\lambda)^2 I(\theta^*) + (1 - r_{\theta^*}^\lambda)^2 \lambda I_d \\
 &\quad (\text{since } 0 < (1 - r_{\theta^*}^\lambda)^2 \leq 1 \text{ and } \lambda I_d \text{ is pos. semidef.}) \\
 &= (1 - r_{\theta^*}^\lambda)^2 (I(\theta^*) + \lambda I_d) = (1 - r_{\theta^*}^\lambda)^2 I_\lambda(\theta^*)
 \end{aligned}$$

Inverting this matrix inequality (using the property that if $A \succeq B \succ 0$, then $B^{-1} \succeq A^{-1} \succ 0$) yields an upper bound on the inverse Hessian:

$$I_\lambda(\theta_\tau)^{-1} \preceq (1 - r_{\theta^*}^\lambda)^{-2} I_\lambda(\theta^*)^{-1}$$

Step 3: Deriving the Final MSE Bound. We substitute the bound on the inverse Hessian back into the MSE expression. Since the bound holds deterministically for a constant $r_{\theta^*}^\lambda$, the term $(1 - r_{\theta^*}^\lambda)^{-2}$ is a constant and can be manipulated outside the expectation.

$$\begin{aligned}
 \mathbb{E}[(\theta_\lambda - \theta^*)(\theta_\lambda - \theta^*)^T] &= \mathbb{E} \left[I_\lambda(\theta_\tau)^{-1} s_\lambda(\theta^*) \times s_\lambda(\theta^*)^\top I_\lambda(\theta_\tau)^{-1} \right] \\
 &\preceq \mathbb{E} \left[(1 - r_{\theta^*}^\lambda)^{-2} I_\lambda(\theta^*)^{-1} s_\lambda(\theta^*) \times s_\lambda(\theta^*)^\top (1 - r_{\theta^*}^\lambda)^{-2} I_\lambda(\theta^*)^{-1} \right] \\
 &= (1 - r_{\theta^*}^\lambda)^{-4} I_\lambda(\theta^*)^{-1} \mathbb{E}[s_\lambda(\theta^*) s_\lambda(\theta^*)^\top] \times I_\lambda(\theta^*)^{-1}
 \end{aligned}$$

Next, we analyze the expectation of the outer product of the regularized score at the true parameter, $\mathbb{E}[s_\lambda(\theta^*) s_\lambda(\theta^*)^\top]$. Let $s(\theta^*)$ be the unregularized score. We know that $\mathbb{E}[s(\theta^*)] = 0$ and $\mathbb{E}[s(\theta^*) s(\theta^*)^\top] = I(\theta^*)$ (by the Information Matrix Equality).

$$\begin{aligned}
 \mathbb{E}[s_\lambda(\theta^*) s_\lambda(\theta^*)^\top] &= \mathbb{E}[(s(\theta^*) - \lambda \theta^*)(s(\theta^*) - \lambda \theta^*)^\top] \\
 &= \mathbb{E}[s(\theta^*) s(\theta^*)^\top] - \lambda \mathbb{E}[s(\theta^*)] (\theta^*)^\top \\
 &\quad - \lambda \theta^* \mathbb{E}[s(\theta^*)^\top] + \lambda^2 \theta^* (\theta^*)^\top \\
 &= I(\theta^*) + \lambda^2 \theta^* (\theta^*)^\top
 \end{aligned}$$

Now invoke Assumption B.2, which gives $\|\theta^*\|_2^2 \leq 1/\lambda$ and implies $\lambda^2 \theta^* (\theta^*)^\top \preceq \lambda I_d$. Using this, we bound the expected score term:

$$\begin{aligned}
 \mathbb{E}[s_\lambda(\theta^*) s_\lambda(\theta^*)^\top] &= I(\theta^*) + \lambda^2 \theta^* (\theta^*)^\top \\
 &\preceq I(\theta^*) + \lambda I_d \\
 &= I_\lambda(\theta^*)
 \end{aligned}$$

Finally, substituting this back into the MSE expression gives the result:

$$\begin{aligned}
 \mathbb{E}[(\theta_\lambda - \theta^*)(\theta_\lambda - \theta^*)^T] &\preceq (1 - r_{\theta^*}^\lambda)^{-4} I_\lambda(\theta^*)^{-1} \\
 &\quad \times \mathbb{E}[s_\lambda(\theta^*) s_\lambda(\theta^*)^\top] \\
 &\quad \times I_\lambda(\theta^*)^{-1} \\
 &\preceq (1 - r_{\theta^*}^\lambda)^{-4} I_\lambda(\theta^*)^{-1} I_\lambda(\theta^*) I_\lambda(\theta^*)^{-1} \\
 &= \frac{1}{(1 - r_{\theta^*}^\lambda)^4} I_\lambda(\theta^*)^{-1}
 \end{aligned}$$

This establishes the bound with constant $C_{\theta^*}^\lambda = (1 - r_{\theta^*}^\lambda)^{-4}$, concluding the proof. \square

B.2. Derivation of the Fisher Information Matrix for Multinomial Logistic Regression

The Fisher Information Matrix (FIM) quantifies the amount of information that an observable random variable carries about an unknown parameter θ upon which the probability of the random variable depends. Here, we derive the FIM for a single preference observation within a multinomial logistic regression model.

Consider a single observation where an expert chooses one item from a set of K items. Let $\mathbf{x}_q \in \mathbb{R}^d$ be the feature vector associated with item $q \in \{1, \dots, K\}$. The probability of the expert choosing item q , given the parameter vector $\theta \in \mathbb{R}^d$, is modeled by the softmax function:

$$\begin{aligned} p_q(\theta) &= P(\text{item } q \text{ is chosen} \mid \mathbf{x}_1, \dots, \mathbf{x}_K, \theta) \\ &= \frac{\exp(\theta^\top \mathbf{x}_q)}{\sum_{q'=1}^K \exp(\theta^\top \mathbf{x}_{q'})} \end{aligned}$$

Let y_q be an indicator variable such that $y_q = 1$ if item q is chosen, and $y_q = 0$ otherwise. Note that $\sum_{q=1}^K y_q = 1$. The log-likelihood for this single observation is:

$$\mathcal{L}(\theta) = \sum_{q=1}^K y_q \log p_q(\theta)$$

The score vector, which is the gradient of the log-likelihood with respect to θ , is:

$$S(\theta) = \nabla_\theta \mathcal{L}(\theta) \sum_{q=1}^K y_q \frac{1}{p_q(\theta)} \nabla_\theta p_q(\theta)$$

The gradient of $p_q(\theta)$ is

$$\nabla_\theta p_q(\theta) = p_q(\theta)(\mathbf{x}_q - \bar{\mathbf{x}}(\theta)),$$

where $\bar{\mathbf{x}}(\theta) = \sum_{q'=1}^K p_{q'}(\theta) \mathbf{x}_{q'}$ is the expected feature vector under the current model. Substituting this into the score function:

$$S(\theta) = \sum_{q=1}^K y_q (\mathbf{x}_q - \bar{\mathbf{x}}(\theta)) = \left(\sum_{q=1}^K y_q \mathbf{x}_q \right) - \bar{\mathbf{x}}(\theta)$$

This can also be written as $S(\theta) = \sum_{q=1}^K (y_q - p_q(\theta)) \mathbf{x}_q$.

The Hessian matrix $H(\theta)$ is the matrix of second derivatives of the log-likelihood: $H(\theta) = \nabla_\theta S(\theta)^\top$.

$$\begin{aligned} H(\theta) &= \nabla_\theta \left(\sum_{q=1}^K y_q \mathbf{x}_q - \sum_{q'=1}^K p_{q'}(\theta) \mathbf{x}_{q'} \right)^\top \\ &= -\nabla_\theta \left(\sum_{q'=1}^K p_{q'}(\theta) \mathbf{x}_{q'} \right)^\top \end{aligned}$$

Calculating the derivative:

$$\begin{aligned} \nabla_\theta \left(\sum_{q'=1}^K p_{q'}(\theta) \mathbf{x}_{q'} \right)^\top &= \sum_{q'=1}^K \left((\nabla_\theta p_{q'}(\theta)) \mathbf{x}_{q'}^\top + p_{q'}(\theta) \nabla_\theta \mathbf{x}_{q'}^\top \right) \\ &= \sum_{q'=1}^K p_{q'}(\theta) (\mathbf{x}_{q'} - \bar{\mathbf{x}}(\theta)) \mathbf{x}_{q'}^\top \quad (\text{since } \nabla_\theta \mathbf{x}_{q'}^\top = 0) \\ &= \sum_{q'=1}^K p_{q'}(\theta) \mathbf{x}_{q'} \mathbf{x}_{q'}^\top - \left(\sum_{q'=1}^K p_{q'}(\theta) \mathbf{x}_{q'} \right) \left(\sum_{q''=1}^K p_{q''}(\theta) \mathbf{x}_{q''} \right)^\top = \sum_{q'=1}^K p_{q'}(\theta) \mathbf{x}_{q'} \mathbf{x}_{q'}^\top - \bar{\mathbf{x}}(\theta) \bar{\mathbf{x}}(\theta)^\top \end{aligned}$$

So, the Hessian is:

$$H(\theta) = - \left(\sum_{q'=1}^K p_{q'}(\theta) \mathbf{x}_{q'} \mathbf{x}_{q'}^\top - \bar{\mathbf{x}}(\theta) \bar{\mathbf{x}}(\theta)^\top \right)$$

The Fisher Information Matrix $I(\theta)$ for this single observation is the negative expectation of the Hessian:

$$I(\theta) = -\mathbb{E}[H(\theta)].$$

Since the Hessian $H(\theta)$ as derived here does not depend on the random outcome variables y_q (after simplification using properties of $p_q(\theta)$), the expectation does not change it. Thus:

$$I(\theta) = \sum_{q'=1}^K p_{q'}(\theta) \mathbf{x}_{q'} \mathbf{x}_{q'}^\top - \bar{\mathbf{x}}(\theta) \bar{\mathbf{x}}(\theta)^\top$$

Expanding $\bar{\mathbf{x}}(\theta) = \sum_{q=1}^K p_q(\theta) \mathbf{x}_q$, we have

$$\begin{aligned} \bar{\mathbf{x}}(\theta) \bar{\mathbf{x}}(\theta)^\top &= \left(\sum_{q=1}^K p_q(\theta) \mathbf{x}_q \right) \left(\sum_{q'=1}^K p_{q'}(\theta) \mathbf{x}_{q'} \right)^\top \\ &= \sum_{q,q'} p_q(\theta) p_{q'}(\theta) \mathbf{x}_q \mathbf{x}_{q'}^\top. \end{aligned}$$

Thus, we get

$$\begin{aligned} \bar{\mathbf{x}}(\theta) \bar{\mathbf{x}}(\theta)^\top &= \left(\sum_{q=1}^K p_q(\theta) \mathbf{x}_q \right) \left(\sum_{q'=1}^K p_{q'}(\theta) \mathbf{x}_{q'} \right)^\top \\ &= \sum_{q,q'} p_q(\theta) p_{q'}(\theta) \mathbf{x}_q \mathbf{x}_{q'}^\top. \end{aligned}$$

$$\begin{aligned} \bar{\mathbf{x}}(\theta) \bar{\mathbf{x}}(\theta)^\top &= \left(\sum_{q=1}^K p_q(\theta) \mathbf{x}_q \right) \left(\sum_{q'=1}^K p_{q'}(\theta) \mathbf{x}_{q'} \right)^\top \\ &= \sum_{q,q'} p_q(\theta) p_{q'}(\theta) \mathbf{x}_q \mathbf{x}_{q'}^\top. \end{aligned}$$

the form:

$$\begin{aligned} I(\theta) &= \sum_{q=1}^K p_q(\theta) \mathbf{x}_q \mathbf{x}_q^\top \\ &\quad - \sum_{q,q'} p_q(\theta) p_{q'}(\theta) \mathbf{x}_q \mathbf{x}_{q'}^\top \end{aligned}$$

This expression represents the FIM for one multinomial preference choice. If there are N independent such choices, the total FIM is the sum of the FIMs from each choice. This derivation provides the basis for the FIM expressions used in the subsequent experimental design.

B.3. Expected Fisher Information Objective for PBRL

Our goal is to select K policies, $\pi_{1:K} = (\pi_1, \dots, \pi_K)$, to maximize information about the unknown parameter θ . A classical challenge in Optimal Experimental Design (OED) is that directly optimizing a discrete set of experiments (trajectories in our case) is often intractable (Pukelsheim, 2006; Fedorov & Hackl, 1997). A standard approach in OED is to instead optimize a design measure, which in our policy-based setting corresponds to optimizing over policies and considering the *expected* Fisher Information Matrix (FIM) they induce.

The total expected regularized FIM, $I_{reg}(\pi_{1:K}, \theta)$, for K policies $\pi_{1:K}$ generating T episodes of H steps each is:

$$I_{reg}(\pi_{1:K}, \theta) = T \sum_{h=1}^H I_h(\pi_{1:K}, \theta) + \lambda I_d$$

Here, $I_h(\pi_{1:K}, \theta)$ is the expected FIM contribution from timestep h of a single episode, averaged over the trajectory distributions η_{π_q} induced by each policy π_q . Let s_h^q be the state of trajectory $\tau_q \sim \eta_{\pi_q}$ at step h , and $p(q|h; \tau_{1..K})$ be the softmax probability of preferring state s_h^q from the set of K states $\{s_h^1, \dots, s_h^K\}$ presented at that step. Then $I_h(\pi_{1:K}, \theta)$ is:

$$\begin{aligned} I_h(\pi_{1:K}, \theta) = & \mathbb{E}_{\substack{\tau_q \sim \eta_{\pi_q} \\ q \in [K]}} \left[\sum_{q=1}^K p(q|h) \phi(s_h^q) \phi(s_h^q)^\top \right. \\ & \left. - \sum_{q,q'} p(q|h) p(q'|h) \phi(s_h^q) \phi(s_h^{q'})^\top \right] \end{aligned}$$

The full derivation for a single multinomial choice is in App. B.2.

The ideal experimental design objective is to choose policies $\pi_{1:K}$ to optimize a scalar criterion $s(\cdot)$ of this expected FIM (e.g., D- or A-optimality):

$$\arg \max_{\pi_{1:K}} s(I_{reg}(\pi_{1:K}, \theta)) \quad (9)$$

These challenges are discussed in Sec. 4. We address them using the reformulation and approximation techniques in the main text (Sec. 4.3) and expand them in Sec. B.4 below.

B.4. Reformulation to a Tractable Objective

This section gives the full derivation of the tractable design objective from Sec. 4.3, following the three steps outlined there.

Step 1: Reformulation using State Visitation Measures. We start from the expected regularized FIM in Eq. 9:

$$I_{reg}(\pi_{1:K}, \theta) = T \sum_{h=1}^H I_h(\pi_{1:K}, \theta) + \lambda I_d.$$

The core of the derivation is to reformulate the per-timestep FIM contribution, $I_h(\pi_{1:K}, \theta)$, in terms of state visitation measures. This is formalized by the following lemma.

Lemma B.2. *Let π_1, \dots, π_K be policies with corresponding trajectory distributions $\eta_{\pi_1}, \dots, \eta_{\pi_K}$ and state visitation measures $d_{\pi_1}^h, \dots, d_{\pi_K}^h$. Let $f(s_1, \dots, s_K)$ be any function of a tuple of K states. Assume trajectories τ_1, \dots, τ_K are drawn independently, $\tau_q \sim \eta_{\pi_q}$. Let s_h^q denote the state at timestep h of trajectory τ_q . Then for any fixed h :*

$$\mathbb{E}_{\substack{\tau_q \sim \eta_{\pi_q} \\ q \in [K]}} [f(s_h^1, \dots, s_h^K)] = \mathbb{E}_{\substack{s_q \sim d_{\pi_q}^h \\ q \in [K]}} [f(s_1, \dots, s_K)]$$

where the expectation on the right is taken with respect to states s_1, \dots, s_K drawn independently from the respective state visitation measures at timestep h . The notation $s_q \sim d_{\pi_q}^h$ for $q \in [K]$ implies the joint draw (s_1, \dots, s_K) is from the product distribution $\prod_{q=1}^K d_{\pi_q}^h$.

Proof of Lemma B.2. For a fixed h , we have:

$$\begin{aligned}
 \mathbb{E}_{\substack{\tau_q \sim \eta_{\pi_q} \\ q \in [K]}} [f(s_h^1, \dots, s_h^K)] &= \sum_{\tau_1, \dots, \tau_K \in \mathcal{T}} \left(\prod_{q=1}^K \eta_{\pi_q}(\tau_q) \right) f(s_h^1, \dots, s_h^K) \\
 &= \sum_{\tau_1, \dots, \tau_K \in \mathcal{T}} \left(\prod_{q=1}^K \eta_{\pi_q}(\tau_q) \right) \sum_{s_1, \dots, s_K \in \mathcal{S}} f(s_1, \dots, s_K) \\
 &\quad \times \prod_{q=1}^K \mathbb{I}_{\{s_q = s_h^q\}} \quad (\text{Indicators}) \\
 &= \sum_{s_1, \dots, s_K \in \mathcal{S}} f(s_1, \dots, s_K) \sum_{\tau_1, \dots, \tau_K \in \mathcal{T}} \left(\prod_{q=1}^K \eta_{\pi_q}(\tau_q) \mathbb{I}_{\{s_q = s_h^q\}} \right) \\
 &\quad (\text{Rearrange}) \\
 &= \sum_{s_1, \dots, s_K \in \mathcal{S}} f(s_1, \dots, s_K) \left(\prod_{q=1}^K \sum_{\tau_q \in \mathcal{T}} \eta_{\pi_q}(\tau_q) \mathbb{I}_{\{s_q = s_h^q\}} \right) \\
 &\quad (\text{Factorize over } \tau) \\
 &= \sum_{s_1, \dots, s_K \in \mathcal{S}} f(s_1, \dots, s_K) \left(\prod_{q=1}^K d_{\pi_q}^h(s_q) \right) \quad (\text{Def. of } d_{\pi_q}^h) \\
 &= \mathbb{E}_{\substack{s_q \sim d_{\pi_q}^h \\ q \in [K]}} [f(s_1, \dots, s_K)] \quad (\text{Def. of product expectation})
 \end{aligned}$$

This completes the proof. \square

Using this lemma, the per-timestep expected FIM $I_h(\pi_{1:K}, \theta)$ can be equivalently expressed in terms of state visitation measures. Let $d_{1:K}^h = (d_{\pi_1}^h, \dots, d_{\pi_K}^h)$. The equality $I_h(\pi_{1:K}, \theta) = I_h(d_{1:K}^h, \theta)$ signifies that the problem is now over the space of visitation measures. However, this expression is still dependent on the unknown θ . In particular, invoking Lemma B.2 with the choice

$$f(s_1, \dots, s_K) = \sum_{q=1}^K p(q \mid h; s_{1:K}, \theta) \phi(s_q) \phi(s_q)^\top - \left(\sum_{q=1}^K p(q \mid h; s_{1:K}, \theta) \phi(s_q) \right) \times \left(\sum_{q'=1}^K p(q' \mid h; s_{1:K}, \theta) \phi(s_{q'}) \right)^\top,$$

we obtain the explicit per-step form

$$\begin{aligned}
 I_h(d_{1:K}^h, \theta) &= \mathbb{E}_{\substack{s_q \sim d_{\pi_q}^h \\ q \in [K]}} [f(s_1, \dots, s_K)] \\
 &= \mathbb{E}_{\substack{s_q \sim d_{\pi_q}^h \\ q \in [K]}} \left[\sum_{q=1}^K p(q \mid h; s_{1:K}, \theta) \phi(s_q) \phi(s_q)^\top \right. \\
 &\quad \left. - \left(\sum_{q=1}^K p(q \mid h; s_{1:K}, \theta) \phi(s_q) \right) \right. \\
 &\quad \left. \times \left(\sum_{q'=1}^K p(q' \mid h; s_{1:K}, \theta) \phi(s_{q'}) \right)^\top \right]. \tag{10}
 \end{aligned}$$

Consequently, defining $I_\lambda(d_{1:K}, \theta) = T \sum_{h=1}^H I_h(d_{1:K}^h, \theta) + \lambda I_d$, the Step 1 design problem reads

$$\arg \max_{d_{1:K} \in \mathcal{D}_{sv}} s(I_\lambda(d_{1:K}, \theta)), \tag{11}$$

where \mathcal{D}_{sv} denotes the set of valid collections of visitation measures. This formulation (still) carries the K -tuple coupling through $p(\cdot | h; s_{1:K}, \theta)$ and depends on the unknown θ , hence it remains computationally challenging and motivates the subsequent steps.

Step 2: θ -agnostic approximation. The per-step information $I_h(d_{1:K}^h, \theta)$ depends on θ only through the softmax probabilities $p(\cdot)$. To design queries without a reliable prior—and avoid brittleness to misspecification—we adopt a symmetric average-case surrogate that is standard in fixed-design OED: replace $p(q | h; s_{1:K}, \theta)$ by its expectation under a symmetric, uninformative prior. This yields

$$p(q | s_{1:K}) \approx \frac{1}{K}.$$

For $K = 2$, this equality holds for any symmetric prior; for $K > 2$, it is a common and reasonable θ -agnostic approximation when the K alternatives are constructed to be diverse/symmetric. It can also be viewed as a homoscedasticity assumption on choice uncertainty when the parameter-dependent heteroscedasticity is unknown (Pukelsheim, 2006). A fully Bayesian alternative—computing $\mathbb{E}_\theta[p(q | h; s_{1:K}, \theta)]$ for every tuple $s_{1:K}$ —is computationally prohibitive at design time.

Substituting the uniform surrogate into $I_h(d_{1:K}^h, \theta)$ yields the approximate expected FIM contribution at timestep h , denoted $\tilde{I}_h(d_{1:K}^h)$, which is now independent of θ :

$$\begin{aligned} \tilde{I}_h(d_{1:K}^h) &= \mathbb{E}_{\substack{s_q \sim d_q^h \\ q \in [K]}} \left[\frac{1}{K} \sum_{q=1}^K \phi(s_q) \phi(s_q)^\top \right. \\ &\quad \left. - \frac{1}{K^2} \sum_{q,q'=1}^K \phi(s_q) \phi(s_{q'})^\top \right] \end{aligned} \quad (12)$$

We denote this per-step quantity by $\tilde{I}_h(d_{1:K}^h)$ throughout; see Eq. 6 in the main text. While now θ -independent, computing this expectation naively still involves a sum over $|\mathcal{S}|^K$ terms.

Step 3: Marginalization for Tractability. Eq. 12 can be marginalized to a tractable closed form, as shown by the theorem below.

Theorem B.3. *Let d_q^h be the state visitation measure for policy π_q at step h , for $q \in [K]$. Under the uniform preference approximation, the expected FIM contribution $\tilde{I}_h(d_{1:K}^h)$ can be rewritten as:*

$$\begin{aligned} \tilde{I}_h(d_{1:K}^h) &= \frac{1}{K} \sum_{q=1}^K \sum_{s \in \mathcal{S}} d_q^h(s) \phi(s) \phi(s)^\top \\ &\quad - \frac{1}{K^2} \sum_{q,q'=1}^K \left(\sum_{s \in \mathcal{S}} d_q^h(s) \phi(s) \right) \left(\sum_{s' \in \mathcal{S}} d_{q'}^h(s') \phi(s')^\top \right) \end{aligned}$$

Furthermore, in matrix notation, where $\Phi \in \mathbb{R}^{|\mathcal{S}| \times d}$ is the feature matrix, $d_q^h \in \mathbb{R}^{|\mathcal{S}|}$ is the state visitation vector, and $\bar{d}^h = \frac{1}{K} \sum_{q=1}^K d_q^h$ is the average visitation vector:

$$\tilde{I}_h(d_{1:K}^h) = \Phi^T \left(\frac{1}{K} \sum_{q=1}^K \text{diag}(d_q^h) - \bar{d}^h (\bar{d}^h)^T \right) \Phi \quad (13)$$

Proof of Theorem B.3. We start with the definition of $\tilde{I}_h(d_{1:K}^h)$ under the uniform approximation from Eq. 12. Let $A_h = \mathbb{E} \left[\frac{1}{K} \sum_{q=1}^K \phi(s_q) \phi(s_q)^\top \right]$ and

$$B_h = \mathbb{E} \left[\frac{1}{K^2} \sum_{q,q'=1}^K \phi(s_q) \phi(s_{q'})^\top \right].$$

By linearity of expectation:

$$\begin{aligned} A_h &= \frac{1}{K} \sum_{q=1}^K \mathbb{E}[\phi(s_q) \phi(s_q)^\top] \\ &= \frac{1}{K} \sum_{q=1}^K \sum_{s \in \mathcal{S}} d_q^h(s) \phi(s) \phi(s)^\top. \end{aligned}$$

For B_h , since s_q and $s_{q'}$ are independent for $q \neq q'$:

$$\begin{aligned} B_h &= \frac{1}{K^2} \sum_{q,q'=1}^K \mathbb{E}[\phi(s_q) \phi(s_{q'})^\top] \\ &= \frac{1}{K^2} \sum_{q,q'=1}^K \mathbb{E}[\phi(s_q)] \mathbb{E}[\phi(s_{q'})]^\top \\ &= \frac{1}{K^2} \sum_{q,q'=1}^K \left(\sum_{s \in \mathcal{S}} d_q^h(s) \phi(s) \right) \left(\sum_{s' \in \mathcal{S}} d_{q'}^h(s') \phi(s')^\top \right). \end{aligned}$$

This yields the first result. For the matrix form, we use the fact that $\sum_s d_q^h(s) \phi(s) \phi(s)^\top = \Phi^T \text{diag}(d_q^h) \Phi$ and $\sum_s d_q^h(s) \phi(s) = \Phi^T d_q^h$.

$$\begin{aligned} A_h &= \frac{1}{K} \sum_{q=1}^K \Phi^T \text{diag}(d_q^h) \Phi \\ &= \Phi^T \left(\frac{1}{K} \sum_{q=1}^K \text{diag}(d_q^h) \right) \Phi. \\ B_h &= \frac{1}{K^2} \sum_{q,q'=1}^K (\Phi^T d_q^h) (\Phi^T d_{q'}^h)^T \\ &= \Phi^T \left(\left(\frac{1}{K} \sum_q d_q^h \right) \left(\frac{1}{K} \sum_{q'} d_{q'}^h \right)^T \right) \Phi \\ &= \Phi^T (\bar{d}^h) (\bar{d}^h)^T \Phi. \end{aligned}$$

Combining $A_h - B_h$ gives the second result. This completes the proof. \square

This final expression for $\tilde{I}_h(d_{1:K}^h)$ is independent of θ and computationally tractable. Therefore, our practical experimental design objective becomes optimizing a scalar criterion $s(\cdot)$ over the state visitation measures $d_{1:K} = \{d_q^h\}_{q \in [K], h \in [H]}$:

$$\arg \max_{d_{1:K}} s \left(T \cdot \sum_{h=1}^H \tilde{I}_h(d_{1:K}^h) + \lambda I_d \right) \quad (14)$$

The optimization is subject to the constraints that these visitation measures are valid in the given MDP.

B.4.1. INFORMATION DECOMPOSITION AND POLICY DIVERSITY

The tractable objective from Thm. B.3 clarifies what makes an informative experiment in preference-based RL. We examine the core matrix term within the approximate FIM at timestep h :

$$M_h(d_{1:K}^h) = \frac{1}{K} \sum_{q=1}^K \text{diag}(d_q^h) - \bar{d}^h (\bar{d}^h)^T$$

This expression can be interpreted in terms of the statistics of the state visitation distributions. The first term, $\frac{1}{K} \sum_{q=1}^K \text{diag}(d_q^h)$, represents the average of the per-policy state variances (since $\text{diag}(d_q^h)$ captures the variance if states were one-hot encoded). The second term, $\bar{d}^h (\bar{d}^h)^T$, represents the outer product of the average state visitation vector. The structure resembles a covariance matrix: $\mathbb{E}[xx^T] - \mathbb{E}[x] \mathbb{E}[x]^T$. Maximizing a scalar function of

$$\tilde{I}_h(d_{1:K}^h) = \Phi^T M_h(d_{1:K}^h) \Phi$$

encourages policies whose average state visitation behavior exhibits high spread in feature space, after accounting for the variance of the average distribution.

This suggests that the objective implicitly favors diversity among the chosen policies π_1, \dots, π_K . If all policies induce very similar state visitation distributions ($d_q^h \approx \bar{d}^h$ for all q), the term $M_h(d_{1:K}^h)$ might be small. Conversely, if the policies explore distinct regions of the state space, leading to diverse d_q^h vectors, the resulting $M_h(d_{1:K}^h)$ is likely to be larger (in a matrix sense, e.g., larger eigenvalues), contributing more to the information gain.

Lemma B.4 formalizes this intuition via an alternative decomposition of $\tilde{I}_h(d_{1:K}^h)$. Invoking it, we can rewrite the approximate FIM contribution as:

$$\tilde{I}_h(d_{1:K}^h) = \underbrace{\Phi^T \left[\frac{1}{K} \sum_{q=1}^K (\text{diag}(d_q^h) - d_q^h (d_q^h)^T) + \frac{1}{K^2} \sum_{1 \leq i < j \leq K} (d_i^h - d_j^h)(d_i^h - d_j^h)^T \right] \Phi}_{\text{Average Per-Policy State Covariance}} + \underbrace{\frac{1}{K^2} \sum_{1 \leq i < j \leq K} (d_i^h - d_j^h)(d_i^h - d_j^h)^T}_{\text{Average Pairwise Difference (Diversity Term)}}$$

This decomposition separates the information contribution into two components:

Average Per-Policy State Covariance. The first term represents the average of the covariance matrices associated with each policy's state visitation distribution d_q^h . It captures the spread within each policy's behavior at timestep h ; maximizing it encourages policies that individually explore diverse states within their own trajectories.

Average Pairwise Difference (Diversity Term). The second term directly quantifies diversity between policies. It is the sum of outer products of differences between the visitation vectors of all pairs (i, j) . This term is maximized when the distributions d_i^h and d_j^h are distinct, promoting policies that explore complementary regions of the state space.

Therefore, optimizing the approximate FIM objective naturally balances exploring broadly within each policy and ensuring that the set of policies collectively covers different aspects of the state space, maximizing the potential for informative comparisons.

Lemma B.4. *Let $\tilde{I}_h(d_{1:K}^h)$ be the approximate expected Fisher Information Matrix contribution at timestep h under the uniform preference assumption, as in Thm. B.3:*

$$\tilde{I}_h(d_{1:K}^h) = \Phi^T \left(\frac{1}{K} \sum_{q=1}^K \text{diag}(d_q^h) - \bar{d}^h (\bar{d}^h)^T \right) \Phi$$

where $d_q^h \in \mathbb{R}^{|\mathcal{S}|}$ is the state visitation vector for policy π_q at step h , $\Phi \in \mathbb{R}^{|\mathcal{S}| \times d}$ is the feature matrix, and $\bar{d}^h = \frac{1}{K} \sum_{q=1}^K d_q^h$. This can be rewritten in terms of pairwise differences between state visitation vectors as:

$$\begin{aligned} \tilde{I}_h(d_{1:K}^h) &= \Phi^T \left[\frac{1}{K} \sum_{q=1}^K (\text{diag}(d_q^h) - d_q^h (d_q^h)^T) \right. \\ &\quad \left. + \frac{1}{K^2} \sum_{1 \leq i < j \leq K} (d_i^h - d_j^h)(d_i^h - d_j^h)^T \right] \Phi \end{aligned}$$

Proof. We start from Thm. B.3. Let $M_h(d_{1:K}^h)$ denote the matrix expression within $\Phi^T(\dots)\Phi$:

$$M_h(d_{1:K}^h) = \frac{1}{K} \sum_{q=1}^K \text{diag}(d_q^h) - \bar{d}^h (\bar{d}^h)^T$$

Expand the outer product of the average state visitation vector:

$$\begin{aligned}\bar{d}^h(\bar{d}^h)^T &= \left(\frac{1}{K} \sum_{i=1}^K d_i^h \right) \left(\frac{1}{K} \sum_{j=1}^K d_j^h \right)^T \\ &= \frac{1}{K^2} \sum_{i=1}^K \sum_{j=1}^K d_i^h (d_j^h)^T\end{aligned}$$

Substitute this into the expression for $M_h(d_{1:K}^h)$:

$$\begin{aligned}M_h(d_{1:K}^h) &= \frac{1}{K} \sum_{q=1}^K \text{diag}(d_q^h) \\ &\quad - \frac{1}{K^2} \sum_{i=1}^K \sum_{j=1}^K d_i^h (d_j^h)^T\end{aligned}$$

We split the double summation based on whether the indices are equal ($i = j$) or distinct ($i \neq j$):

$$\sum_{i=1}^K \sum_{j=1}^K d_i^h (d_j^h)^T = \sum_{q=1}^K d_q^h (d_q^h)^T + \sum_{i \neq j} d_i^h (d_j^h)^T$$

Substituting this yields:

$$\begin{aligned}M_h(d_{1:K}^h) &= \frac{1}{K} \sum_{q=1}^K \text{diag}(d_q^h) - \frac{1}{K^2} \sum_{q=1}^K d_q^h (d_q^h)^T \\ &\quad - \frac{1}{K^2} \sum_{i \neq j} d_i^h (d_j^h)^T\end{aligned}$$

By adding and subtracting the term $(K - 1) \frac{1}{K^2} \sum_{q=1}^K d_q^h (d_q^h)^T$:

$$\begin{aligned}M_h(d_{1:K}^h) &= \frac{1}{K} \sum_{q=1}^K \text{diag}(d_q^h) - \frac{1}{K^2} \sum_{q=1}^K d_q^h (d_q^h)^T \\ &\quad - (K - 1) \frac{1}{K^2} \sum_{q=1}^K d_q^h (d_q^h)^T \\ &\quad + (K - 1) \frac{1}{K^2} \sum_{q=1}^K d_q^h (d_q^h)^T - \frac{1}{K^2} \sum_{i \neq j} d_i^h (d_j^h)^T\end{aligned}$$

Combine the terms containing $\sum_{q=1}^K d_q^h (d_q^h)^T$:

$$\begin{aligned}
 M_h(d_{1:K}^h) &= \frac{1}{K} \sum_{q=1}^K \text{diag}(d_q^h) - (1+K-1) \frac{1}{K^2} \sum_{q=1}^K d_q^h (d_q^h)^T \\
 &\quad + \frac{K-1}{K^2} \sum_{q=1}^K d_q^h (d_q^h)^T - \frac{1}{K^2} \sum_{i \neq j} d_i^h (d_j^h)^T \\
 &= \frac{1}{K} \sum_{q=1}^K \text{diag}(d_q^h) - \frac{K}{K^2} \sum_{q=1}^K d_q^h (d_q^h)^T \\
 &\quad + \frac{K-1}{K^2} \sum_{q=1}^K d_q^h (d_q^h)^T - \frac{1}{K^2} \sum_{i \neq j} d_i^h (d_j^h)^T \\
 &= \left(\frac{1}{K} \sum_{q=1}^K \text{diag}(d_q^h) - \frac{1}{K} \sum_{q=1}^K d_q^h (d_q^h)^T \right) \\
 &\quad + \left(\frac{K-1}{K^2} \sum_{q=1}^K d_q^h (d_q^h)^T - \frac{1}{K^2} \sum_{i \neq j} d_i^h (d_j^h)^T \right)
 \end{aligned}$$

Consider the sum of outer products of pairwise differences over unique pairs $\{i, j\}$ such that $1 \leq i < j \leq K$:

$$\begin{aligned}
 &\sum_{1 \leq i < j \leq K} (d_i^h - d_j^h)(d_i^h - d_j^h)^T \\
 &= \sum_{i < j} \left(d_i^h (d_i^h)^T - d_i^h (d_j^h)^T \right. \\
 &\quad \left. - d_j^h (d_i^h)^T + d_j^h (d_j^h)^T \right) \\
 &= (K-1) \sum_{q=1}^K d_q^h (d_q^h)^T \\
 &\quad - \sum_{i < j} (d_i^h (d_j^h)^T + d_j^h (d_i^h)^T)
 \end{aligned}$$

The second term $\sum_{i < j} (d_i^h (d_j^h)^T + d_j^h (d_i^h)^T)$ sums over all distinct pairs $\{i, j\}$, equivalent to the summation $\sum_{i \neq j} d_i^h (d_j^h)^T$. Thus,

$$\begin{aligned}
 &\sum_{1 \leq i < j \leq K} (d_i^h - d_j^h)(d_i^h - d_j^h)^T \\
 &= (K-1) \sum_{q=1}^K d_q^h (d_q^h)^T \\
 &\quad - \sum_{i \neq j} d_i^h (d_j^h)^T
 \end{aligned}$$

Dividing by K^2 yields:

$$\begin{aligned}
 &\frac{1}{K^2} \sum_{1 \leq i < j \leq K} (d_i^h - d_j^h)(d_i^h - d_j^h)^T \\
 &= \frac{K-1}{K^2} \sum_{q=1}^K d_q^h (d_q^h)^T \\
 &\quad - \frac{1}{K^2} \sum_{i \neq j} d_i^h (d_j^h)^T
 \end{aligned}$$

This exactly matches the second grouped term derived for $M_h(d_{1:K}^h)$. Substituting this structure back gives:

$$\begin{aligned}
 M_h(d_{1:K}^h) &= \left(\frac{1}{K} \sum_{q=1}^K \text{diag}(d_q^h) - \frac{1}{K} \sum_{q=1}^K d_q^h (d_q^h)^T \right) \\
 &\quad + \frac{1}{K^2} \sum_{1 \leq i < j \leq K} (d_i^h - d_j^h)(d_i^h - d_j^h)^T \\
 &= \frac{1}{K} \sum_{q=1}^K (\text{diag}(d_q^h) - d_q^h (d_q^h)^T) \\
 &\quad + \frac{1}{K^2} \sum_{1 \leq i < j \leq K} (d_i^h - d_j^h)(d_i^h - d_j^h)^T
 \end{aligned}$$

Finally, reintroducing the outer feature matrix multiplication provides the desired result:

$$\begin{aligned}
 \tilde{I}_h(d_{1:K}^h) &= \Phi^T M_h(d_{1:K}^h) \Phi \\
 &= \Phi^T \left[\frac{1}{K} \sum_{q=1}^K (\text{diag}(d_q^h) - d_q^h (d_q^h)^T) \right. \\
 &\quad \left. + \frac{1}{K^2} \sum_{1 \leq i < j \leq K} (d_i^h - d_j^h)(d_i^h - d_j^h)^T \right] \Phi
 \end{aligned}$$

□

B.5. Formal: Relationship between the State-based Feedback model and the Truncated Feedback model

We now formally analyze the relationship between the information content of the State-based feedback model and the Truncated Trajectory feedback model. This analysis is performed under the *perfect decomposition condition*, where the features of a truncated trajectory are assumed to be the sum of the features of its constituent states. We also use the uniform preference approximation ($p(q|s_{1..K}) \approx 1/K$) from Step 2 of Sec. 4.3 (Eq. 12). This yields the following θ -independent structure for the approximated Fisher Information matrix component, \tilde{I}_h , derived from comparing K feature vectors $\{\mathbf{x}_q\}_{q=1}^K$ at a given step h :

$$\begin{aligned}
 \tilde{I}_h(\mathbf{x}_1, \dots, \mathbf{x}_K) &= \frac{1}{K} \sum_{q=1}^K \mathbf{x}_q \mathbf{x}_q^\top \\
 &\quad - \frac{1}{K^2} \sum_{q,q'=1}^K \mathbf{x}_q \mathbf{x}_{q'}^\top
 \end{aligned}$$

The following theorem compares the approximated FIMs of the two models under these conditions.

Theorem B.5 (Comparison of Approximated FIMs). *Let $\mathcal{T}^K = \{(\tau_t^1, \dots, \tau_t^K)\}_{t=1}^T$ be a set of $T \times K$ trajectories. For the standard (state-based) feedback model, let $\phi(s_{t,h}^q)$ be the feature vector for the state $s_{t,h}^q$. The approximated Fisher Information Matrix is*

$$\begin{aligned}
 \tilde{I}^{\text{state}}(\mathcal{T}^K) &= \sum_{t=1}^T \sum_{h=1}^H \left(\frac{1}{K} \sum_{q=1}^K \phi(s_{t,h}^q) \phi(s_{t,h}^q)^\top \right. \\
 &\quad \left. - \frac{1}{K^2} \sum_{q,q'=1}^K \phi(s_{t,h}^q) \phi(s_{t,h}^{q'})^\top \right).
 \end{aligned}$$

For the truncated trajectory feedback model, assume the perfect decomposition condition holds, such that the feature representation of the q -th trajectory in episode t truncated at timestep h is $\psi_{t,h}^q = \sum_{h'=1}^h \phi(s_{t,h'}^q)$. The corresponding

approximated Fisher Information Matrix is

$$\tilde{I}^{trunc}(\mathcal{T}^K) = \sum_{t=1}^T \sum_{h=1}^H \left(\frac{1}{K} \sum_{q=1}^K \psi_{t,h}^q (\psi_{t,h}^q)^\top - \frac{1}{K^2} \sum_{q,q'=1}^K \psi_{t,h}^q (\psi_{t,h}^{q'})^\top \right).$$

Then, under the perfect decomposition condition,

$$\tilde{I}^{trunc}(\mathcal{T}^K) \succeq \frac{1}{4} \cdot \tilde{I}^{state}(\mathcal{T}^K).$$

Proof of Theorem B.5. Let $\mathcal{T}^K = \{(\tau_t^1, \dots, \tau_t^K)\}_{t=1}^T$ be the set of trajectories. We define two approximated Fisher Information Matrices based on the uniform preference assumption ($p \approx 1/K$).

First, the FIM for the state-based feedback model, denoted $I_{approx}^{state}(\mathcal{T}^K)$, uses features $\phi(s_{t,h}^q)$ from individual states:

$$I_{approx}^{state}(\mathcal{T}^K) = \sum_{t=1}^T \sum_{h=1}^H \left(\frac{1}{K} \sum_{q=1}^K \phi(s_{t,h}^q) \phi(s_{t,h}^q)^\top - \frac{1}{K^2} \sum_{q,q'=1}^K \phi(s_{t,h}^q) \phi(s_{t,h}^{q'})^\top \right).$$

Next, the FIM for the truncated trajectory feedback model, $I_{approx}^{trunc}(\mathcal{T}^K)$, under the perfect decomposition condition, uses the sum-decomposed features $\psi_{t,h}^q = \sum_{h'=1}^h \phi(s_{t,h'}^q)$:

$$I_{approx}^{trunc}(\mathcal{T}^K) = \sum_{t=1}^T \sum_{h=1}^H \left(\frac{1}{K} \sum_{q=1}^K \psi_{t,h}^q (\psi_{t,h}^q)^\top - \frac{1}{K^2} \sum_{q,q'=1}^K \psi_{t,h}^q (\psi_{t,h}^{q'})^\top \right).$$

Let $\Phi_{t,q} \in \mathbb{R}^{H \times d}$ be the matrix whose h -th row is $\phi(s_{t,h}^q)^\top$. That is,

$$\Phi_{t,q} = \begin{pmatrix} \phi(s_{t,1}^q)^\top \\ \phi(s_{t,2}^q)^\top \\ \vdots \\ \phi(s_{t,H}^q)^\top \end{pmatrix}.$$

The sum of outer products over the horizon H for the state-based model is

$$\sum_{h=1}^H \phi(s_{t,h}^q) \phi(s_{t,h}^q)^\top = \Phi_{t,q}^\top I_H \Phi_{t,q},$$

where I_H is the $H \times H$ identity matrix. Similarly, the sum of cross-products is

$$\sum_{h=1}^H \phi(s_{t,h}^q) \phi(s_{t,h}^{q'})^\top = \Phi_{t,q}^\top I_H \Phi_{t,q'}.$$

Thus, $\tilde{I}^{\text{state}}(\mathcal{T}^K)$ can be rewritten as:

$$\begin{aligned}\tilde{I}^{\text{state}}(\mathcal{T}^K) &= \sum_{t=1}^T \left(\frac{1}{K} \sum_{q=1}^K \Phi_{t,q}^\top I_H \Phi_{t,q} \right. \\ &\quad \left. - \frac{1}{K^2} \sum_{q,q'=1}^K \Phi_{t,q}^\top I_H \Phi_{t,q'} \right).\end{aligned}$$

For the truncated trajectory model (under perfect decomposition), let $\Psi_{t,q} \in \mathbb{R}^{H \times d}$ be the matrix whose h -th row is $(\psi_{t,h}^q)^\top = \left(\sum_{h'=1}^h \phi(s_{t,h'}^q) \right)^\top$. Let $S \in \mathbb{R}^{H \times H}$ be the lower triangular matrix of ones, i.e., $S_{ij} = 1$ if $i \geq j$ and $S_{ij} = 0$ if $i < j$. For example, if $H = 3$:

$$S = \begin{pmatrix} 1 & 0 & 0 \\ 1 & 1 & 0 \\ 1 & 1 & 1 \end{pmatrix}.$$

The cumulative sum structure means $\Psi_{t,q} = S\Phi_{t,q}$. The sum of outer products over the horizon H for the truncated model is

$$\begin{aligned}\sum_{h=1}^H \psi_{t,h}^q (\psi_{t,h}^q)^\top &= \Psi_{t,q}^\top \Psi_{t,q} = (S\Phi_{t,q})^\top (S\Phi_{t,q}) \\ &= \Phi_{t,q}^\top S^\top S \Phi_{t,q}.\end{aligned}$$

Similarly, the sum of cross-products is

$$\begin{aligned}\sum_{h=1}^H \psi_{t,h}^q (\psi_{t,h}^{q'})^\top &= \Psi_{t,q}^\top \Psi_{t,q'} \\ &= \Phi_{t,q}^\top S^\top S \Phi_{t,q'}.\end{aligned}$$

Let $M = S^\top S$. This is an $H \times H$ symmetric positive definite matrix. For $H = 3$,

$$\begin{aligned}M &= S^\top S \\ &= \begin{pmatrix} 1 & 1 & 1 \\ 0 & 1 & 1 \\ 0 & 0 & 1 \end{pmatrix} \begin{pmatrix} 1 & 0 & 0 \\ 1 & 1 & 0 \\ 1 & 1 & 1 \end{pmatrix} \\ &= \begin{pmatrix} 3 & 2 & 1 \\ 2 & 2 & 1 \\ 1 & 1 & 1 \end{pmatrix}.\end{aligned}$$

Thus, $\tilde{I}^{\text{trunc}}(\mathcal{T}^K)$ can be expressed in terms of $\Phi_{t,q}$ and M :

$$\begin{aligned}\tilde{I}^{\text{trunc}}(\mathcal{T}^K) &= \sum_{t=1}^T \left(\frac{1}{K} \sum_{q=1}^K \Phi_{t,q}^\top M \Phi_{t,q} \right. \\ &\quad \left. - \frac{1}{K^2} \sum_{q,q'=1}^K \Phi_{t,q}^\top M \Phi_{t,q'} \right).\end{aligned}$$

Let

$$X_t = (\Phi_{t,1}^\top \dots \Phi_{t,K}^\top)^\top \in \mathbb{R}^{(KH) \times d}.$$

Let $J_K = \frac{1}{K} \mathbf{1}_K \mathbf{1}_K^\top$ be the $K \times K$ matrix of all $1/K$. Let I_K be the $K \times K$ identity matrix. The FIM expressions can be written compactly using Kronecker products \otimes :

$$\begin{aligned}\tilde{I}^{\text{state}}(\mathcal{T}^K) &= \sum_{t=1}^T X_t^\top \left(\frac{1}{K} (I_K - J_K) \otimes I_H \right) X_t \\ \tilde{I}^{\text{trunc}}(\mathcal{T}^K) &= \sum_{t=1}^T X_t^\top \left(\frac{1}{K} (I_K - J_K) \otimes M \right) X_t\end{aligned}$$

Since $M = S^\top S$ is positive definite (as S is invertible), its eigenvalues are positive. Let $\lambda_{\min}(M)$ be the smallest eigenvalue of M . Then $M \succeq \lambda_{\min}(M) I_H$. The matrix $I_K - J_K$ is positive semidefinite (it's proportional to a projection matrix). Therefore, using properties of Kronecker products and Loewner order:

$$\begin{aligned}(I_K - J_K) \otimes M &\succeq (I_K - J_K) \otimes (\lambda_{\min}(M) I_H) \\ &= \lambda_{\min}(M) (I_K - J_K) \otimes I_H\end{aligned}$$

Multiplying by $1/K$ and summing over t after pre- and post-multiplying by X_t^\top and X_t :

$$\begin{aligned}\sum_{t=1}^T X_t^\top \left(\frac{1}{K} (I_K - J_K) \otimes M \right) X_t \\ \succeq \lambda_{\min}(M) \sum_{t=1}^T X_t^\top \left(\frac{1}{K} (I_K - J_K) \otimes I_H \right) X_t\end{aligned}$$

This shows $\tilde{I}^{\text{trunc}}(\mathcal{T}^K) \succeq \lambda_{\min}(M) \cdot \tilde{I}^{\text{state}}(\mathcal{T}^K)$. The eigenvalues of $M = S^\top S$ are known to be

$$\lambda_k(M) = \frac{1}{4 \sin^2 \left(\frac{(2k-1)\pi}{2(2H+1)} \right)}, \quad k = 1, \dots, H.$$

Since $\sin^2(x) \leq 1$ for any x , the minimum eigenvalue $\lambda_{\min}(M)$ is lower-bounded by $1/4$. Therefore, we can state the result using this constant lower bound:

$$\tilde{I}^{\text{trunc}}(\mathcal{T}^K) \succeq \frac{1}{4} \cdot \tilde{I}^{\text{state}}(\mathcal{T}^K)$$

This completes the proof. \square

B.6. Detailed Algorithm Description

ED-PBRL (Alg. 2) has two phases. Phase 1 optimizes K policies using Convex-RL for the objective in Sec. 4.3. Phase 2 executes these policies to collect K sets of trajectories for preference feedback.

Phase 1: Compute Optimal State Visitation Measures This phase adapts the Frank-Wolfe algorithm (Frank & Wolfe, 1956) to maximize $s(I_{\text{total}}(\pi_{1:K}))$. Here, $I_{\text{total}}(\pi_{1:K})$ is the total approximate expected regularized FIM (the matrix argument of $s(\cdot)$ in Eq. 7), expressed via policy-induced visitation measures. We iteratively build state-action visitation measures $\{(^{(n)}d_{\text{mix},q}^h\}$ corresponding to conceptual mixture policies, starting from $^{(1)}d_{\text{mix},q} = \mathbf{0}$.

Each iteration n of this phase involves these main steps:

- Gradient Computation:** The gradient of $s(I_{\text{total}})$ (using the current $^{(n)}d_{\text{mix},q}$) defines a reward function r_{grad_q} for each policy q .
- Policy Search Oracle:** For each q , a new base policy $\pi_{\text{grad}_q}^{(n)}$ is found by maximizing the expected cumulative reward r_{grad_q} (e.g., via value iteration). Its visitation measure $d_{\text{grad}_q}^{(n)}$ is computed.
- Line Search for Step Size:** The optimal step size α_n is determined by maximizing $s(\cdot)$ for the candidate mixture $(1 - \alpha_n)^{^{(n)}d_{\text{mix},q}} + \alpha_n d_{\text{grad}_q}^{(n)}$.

Algorithm 2 ED-PBRL using Convex-RL (Detailed Version of Algorithm 1)

Input: Known MDP components $M = (\mathcal{S}, \mathcal{A}, P, H, \rho)$, number of policies K , number of episodes T , feature map Φ , scalar criterion $s(\cdot)$, number of optimization iterations N , regularization constant λ ($\lambda > 0$)

Output: Estimated preference parameter $\hat{\theta}$

Phase 1: Compute Optimal State Visitation Measures {Solve (7)}

Initialize ${}^{(1)}d_{\text{mix},q}^{\{1,\dots,H\}} \leftarrow \mathbf{0}$ for $q = 1, \dots, K$ {Initialize visitation measures}

for $n = 1$ **to** $N - 1$ **do**

 Let $I_{\text{total}}^{(n)} = T \sum_{h=1}^H \tilde{I}_h({}^{(n)}d_{\text{mix},1:K}^h) + \lambda I_d$ {Objective using ${}^{(n)}d_{\text{mix}}$ }

for $q = 1$ **to** K **do**

 Compute gradient reward: $r_{\text{grad},q}(h, s, a) \leftarrow \nabla_{d_{\pi_q}^h(s,a)} s(I_{\text{total}}^{(n)})$

 Find policy maximizing linear objective: $\pi_{\text{grad},q}^{(n)} \leftarrow \text{value_iteration}(M, r_{\text{grad},q})$

 Compute corresponding visitation vector $d_{\text{grad},q}^{(n),\{1,\dots,H\}}$ from $\pi_{\text{grad},q}^{(n)}$

end for

 Determine step size α_n via line search: For $q = 1, \dots, K$, let $d_{\text{cand},q}^h(\alpha') = (1 - \alpha') {}^{(n)}d_{\text{mix},q}^h + \alpha' d_{\text{grad},q}^{(n),h}$.

 Find $\alpha_n \leftarrow \arg \max_{\alpha' \in [0,1]} s\left(T \sum_{h=1}^H \tilde{I}_h(d_{\text{cand},1:K}^h(\alpha')) + \lambda I_d\right)$.

for $q = 1$ **to** K **do**

${}^{(n+1)}d_{\text{mix},q}^{\{1,\dots,H\}} \leftarrow (1 - \alpha_n) \cdot {}^{(n)}d_{\text{mix},q}^{\{1,\dots,H\}} + \alpha_n \cdot d_{\text{grad},q}^{(n),\{1,\dots,H\}}$

end for

end for

Let $\{d_{\text{mix},q}^h\}_{h,q} \leftarrow \{{}^{(N)}d_{\text{mix},q}^{\{1,\dots,H\}}\}_{h,q}$ be the final optimal visitation measures.

Phase 2: Policy Extraction and Trajectory Sampling

for $q = 1$ **to** K **do**

 Extract policy π_q^* from final visitation measure $d_{\text{mix},q}^{*h}$

$\mathcal{T}_q \leftarrow \emptyset$ {Initialize trajectory set for policy π_q^* }

end for

for $t = 1$ **to** T **do**

for $q = 1$ **to** K **do**

 Sample trajectory $\tau_t^q \sim \pi_q^*$

$\mathcal{T}_q \leftarrow \mathcal{T}_q \cup \{\tau_t^q\}$

end for

end for

Let $\mathcal{D}_{\text{feedback}} = \{\mathcal{T}_q\}_{q=1}^K$ be the collected trajectories.

Phase 3: Parameter Estimation

Collect preference feedback for trajectories in $\mathcal{D}_{\text{feedback}}$.

Estimate $\hat{\theta}$ using all collected feedback (see Sec. 3).

return $\hat{\theta}$

4. **Mixture Update:** The next mixture's visitation measure is constructed:

$${}^{(n+1)}d_{\text{mix},q} \leftarrow (1 - \alpha_n) {}^{(n)}d_{\text{mix},q} + \alpha_n d_{\text{grad}_q}^{(n)}.$$

This efficiently computes the visitation measure of the new conceptual mixture policy $\pi_{\text{mix},q}^{(n)}$.

This iterative process converges to the globally optimal visitation measures $\{d_{\text{mix},q}^{*h}\}$ due to the concavity of $s(\cdot)$ and the convexity of the feasible set of visitation measures.

Phase 2: Policy Extraction and Trajectory Sampling Upon convergence of Phase 1 after $N - 1$ iterations, the final policies $\{\pi_q^*\}_{q=1}^K$ are extracted from the resulting state-action visitation measures $\{d_{\text{mix},q}^{*h}\}_{q=1}^K$. These policies are then executed to generate the $K \times T$ trajectories, which form the dataset $\mathcal{D}_{\text{feedback}}$ for collecting user preference feedback.

Phase 3: Parameter Estimation After the trajectories are generated and collected into $\mathcal{D}_{\text{feedback}}$ in Phase 2, preference feedback is obtained from the user. This accumulated feedback is then used to compute the final estimate $\hat{\theta}$ of the true reward parameter θ , as detailed in Sec. 3.

B.7. Detailed Theoretical Guarantees

The Convex-RL optimization phase (Alg. 2, lines 13-24) employs the Frank-Wolfe (conditional gradient) method over the convex polytope of valid state-action visitation measures (Puterman, 2014; Frank & Wolfe, 1956; Jaggi, 2013). The exact line search for the step size α_n is a standard Frank-Wolfe variant.

The key to guaranteeing global optimality is the concavity of the objective. Let $D = \{d_q^h\}_{h \in [H], q \in [K]}$ be the collection of state visitation vectors, with each $d_q^h \in \Delta^{|\mathcal{S}|-1}$. The domain of D is convex. The objective is $f(D) = s(I_{\text{total}}(D))$, where $I_{\text{total}}(D)$ is the matrix argument of $s(\cdot)$ in Eq. 7:

$$\begin{aligned} I_{\text{total}}(D) = T \sum_{h=1}^H & \left[\Phi^T \left(\frac{1}{K} \sum_{q=1}^K \text{diag}(d_q^h) \right. \right. \\ & \left. \left. - \left(\frac{1}{K} \sum_{q=1}^K d_q^h \right) \left(\frac{1}{K} \sum_{q=1}^K d_q^h \right)^T \right) \Phi \right] + \lambda I_d. \end{aligned}$$

With concavity established (Thm. 5.1), we can state the convergence guarantee for Alg. 2 (Thm. B.6).

B.7.1. PROOF OF OBJECTIVE CONCAVITY (THM. 5.1)

Theorem 5.1. *Let $d_{1:K} = \{d_q^h\}_{h \in [H], q \in [K]}$. If the scalarization $s : \mathbb{S}_+^d \rightarrow \mathbb{R}$ is concave and matrix-monotone, then $(I_{\text{total}}(d_{1:K}))$ as defined in (7) is concave in $d_{1:K}$.*

Proof. Let $D = \{d_q^h\}_{h \in [H], q \in [K]}$ be the collection of state visitation vectors, where each $d_q^h \in \Delta^{|\mathcal{S}|-1}$ (the probability simplex in $\mathbb{R}^{|\mathcal{S}|}$). The domain of D , denoted \mathcal{D}_{sv} , is a Cartesian product of simplices, which is a convex set. The objective function is $f(D) = s(I_{\text{total}}(D))$, where

$$I_{\text{total}}(D) = T \sum_{h=1}^H \tilde{I}_h(D^h) + \lambda I_d,$$

which matches Eq. 7 in the main text. and $D^h = (d_1^h, \dots, d_K^h)$ are the visitation vectors for timestep h . The term $\tilde{I}_h(D^h)$ is given by:

$$\begin{aligned} \tilde{I}_h(D^h) &= \Phi^T M_h(D^h) \Phi, \\ M_h(D^h) &= \frac{1}{K} \sum_{q=1}^K \text{diag}(d_q^h) - \left(\frac{1}{K} \sum_{q=1}^K d_q^h \right) \left(\frac{1}{K} \sum_{q=1}^K d_q^h \right)^T. \end{aligned}$$

We will prove the concavity of $f(D)$ by showing that $I_{total}(D)$ is a concave matrix-valued function of D , and then using the properties of $s(\cdot)$.

1. Concavity of $M_h(D^h)$: Let $L_h(D^h) = \frac{1}{K} \sum_{q=1}^K \text{diag}(d_q^h)$. The function $\text{diag}(v)$ is a linear mapping from a vector v to a diagonal matrix. Thus, $L_h(D^h)$ is a linear function of the collection of vectors $D^h = (d_1^h, \dots, d_K^h)$. Linear functions are both concave and convex.

Let $\bar{d}^h(D^h) = \frac{1}{K} \sum_{q=1}^K d_q^h$. This is also a linear function of D^h . Consider the function $Q(v) = -vv^T$. The function $v \mapsto vv^T$ is convex. To see this, for v_1, v_2 and $\alpha \in [0, 1]$:

$$\begin{aligned}
 & \alpha v_1 v_1^T + (1 - \alpha) v_2 v_2^T \\
 & - (\alpha v_1 + (1 - \alpha) v_2)(\alpha v_1 + (1 - \alpha) v_2)^T \\
 & = \alpha v_1 v_1^T + (1 - \alpha) v_2 v_2^T \\
 & - (\alpha^2 v_1 v_1^T + \alpha(1 - \alpha)(v_1 v_2^T + v_2 v_1^T) \\
 & + (1 - \alpha)^2 v_2 v_2^T) \\
 & = (\alpha - \alpha^2) v_1 v_1^T \\
 & + ((1 - \alpha) - (1 - \alpha)^2) v_2 v_2^T \\
 & - \alpha(1 - \alpha)(v_1 v_2^T + v_2 v_1^T) \\
 & = \alpha(1 - \alpha) v_1 v_1^T + \alpha(1 - \alpha) v_2 v_2^T \\
 & - \alpha(1 - \alpha)(v_1 v_2^T + v_2 v_1^T) \\
 & = \alpha(1 - \alpha)(v_1 - v_2)(v_1 - v_2)^T.
 \end{aligned}$$

Since $\alpha(1 - \alpha) \geq 0$ and $(v_1 - v_2)(v_1 - v_2)^T \succeq 0$ (it's an outer product, hence positive semidefinite), the expression is $\succeq 0$. Thus, $v \mapsto vv^T$ is convex. Therefore, $Q(v) = -vv^T$ is concave. The composition of a concave function with a linear function is concave. Since $Q(v)$ is concave and $\bar{d}^h(D^h)$ is linear, the function $D^h \mapsto Q(\bar{d}^h(D^h)) = -\bar{d}^h(D^h)(\bar{d}^h(D^h))^T$ is concave.

$M_h(D^h) = L_h(D^h) + Q(\bar{d}^h(D^h))$ is the sum of a linear function (which is concave) and a concave function. Thus, $M_h(D^h)$ is a concave matrix-valued function of D^h .

2. Concavity of $\tilde{I}_h(D^h)$: The function $\tilde{I}_h(D^h) = \Phi^T M_h(D^h) \Phi$ is a congruence transformation of $M_h(D^h)$. Since $M_h(D^h)$ is concave in D^h , and congruence transformations preserve concavity (i.e., if $A(x)$ is concave, then $C^T A(x) C$ is concave for any constant matrix C), $\tilde{I}_h(D^h)$ is concave in D^h .

3. Concavity of $I_{total}(D)$: The total approximate FIM before regularization is $\sum_{h=1}^H \tilde{I}_h(D^h)$. Since each $\tilde{I}_h(D^h)$ is concave with respect to its arguments D^h (and thus with respect to the full D , as it doesn't depend on $D^{h'}$ for $h' \neq h$), their sum is concave with respect to D . Multiplying by a non-negative scalar T preserves concavity. So, $T \sum_{h=1}^H \tilde{I}_h(D^h)$ is concave in D . Adding a constant matrix λI_d also preserves concavity. Therefore, $I_{total}(D) = T \sum_{h=1}^H \tilde{I}_h(D^h) + \lambda I_d$ is a concave matrix-valued function of D .

4. Concavity of $s(I_{total}(D))$: We are given that the scalar criterion $s : \mathbb{S}_+^d \rightarrow \mathbb{R}$ is concave and matrix-monotone non-decreasing. If $g(x)$ is matrix-valued concave and $s(A)$ is scalar-valued concave and non-decreasing in A (Loewner order), then $s(g(x))$ is concave (see Boyd & Vandenberghe, Convex Optimization, Sec. 3.2.4). In our case, $g(D) = I_{total}(D)$ is concave in D . Thus, $f(D) = s(I_{total}(D))$ is concave with respect to $D = \{d_q^h\}_{h \in [H], q \in [K]}$ over the convex domain \mathcal{D}_{sv} . \square

B.7.2. PROOF OF CONVERGENCE GUARANTEE (THM. B.6)

Theorem B.6. [Convergence Guarantee (Detailed)] Let $D^{(n)}$ be the sequence of collections of state visitation measures generated by Algorithm 2, where $D^{(1)}$ is the initialization and $D^{(n+1)}$ is the iterate after n Frank-Wolfe steps. Let $f(D) = s(I_{total}(D))$ be the objective function defined in Theorem 5.1, and let $D^* \in \mathcal{D}_{sv}$ be an optimal solution, $D^* = \arg \max_{D \in \mathcal{D}_{sv}} f(D)$. The domain \mathcal{D}_{sv} of valid collections of state visitation measures is compact and convex. If Algorithm 2 performs N_{iter} iterations of the Frank-Wolfe update (i.e., the loop from $n = 1$ to N_{iter} in the algorithm's

notation, resulting in the final iterate $D^{(N_{iter}+1)}$, using exact line search for α_n at each iteration, then the suboptimality of the final iterate $D^{(N_{iter}+1)}$ is bounded by:

$$f(D^*) - f(D^{(N_{iter}+1)}) \leq \frac{2C_f}{N_{iter} + 2}$$

where C_f is the curvature constant of f over \mathcal{D}_{sv} .

Theorem B.6. [Convergence Guarantee (Detailed)] Let $D^{(n)}$ be the sequence of collections of state visitation measures generated by Algorithm 2, where $D^{(1)}$ is the initialization and $D^{(n+1)}$ is the iterate after n Frank-Wolfe steps. Let $f(D) = s(I_{total}(D))$ be the objective function defined in Theorem 5.1, and let $D^* \in \mathcal{D}_{sv}$ be an optimal solution, $D^* = \arg \max_{D \in \mathcal{D}_{sv}} f(D)$. The domain \mathcal{D}_{sv} of valid collections of state visitation measures is compact and convex. If Algorithm 2 performs N_{iter} iterations of the Frank-Wolfe update (i.e., the loop from $n = 1$ to N_{iter} in the algorithm's notation, resulting in the final iterate $D^{(N_{iter}+1)}$, using exact line search for α_n at each iteration, then the suboptimality of the final iterate $D^{(N_{iter}+1)}$ is bounded by:

$$f(D^*) - f(D^{(N_{iter}+1)}) \leq \frac{2C_f}{N_{iter} + 2}$$

where C_f is the curvature constant of f over \mathcal{D}_{sv} .

Proof. The convergence of Algorithm 2 relies on standard results for the Frank-Wolfe algorithm when maximizing a concave function over a compact convex set. We verify the conditions required for these guarantees.

1. Objective Function and Domain:

- **Concavity:** The objective function $f(D) = s(I_{total}(D))$ is concave with respect to the collection of state visitation vectors $D = \{d_q^h\}_{h,q}$, as proven in Theorem 5.1.
- **Domain \mathcal{D}_{sv} :** The domain \mathcal{D}_{sv} is the set of all valid collections of state visitation measures $\{d_q^h\}_{h,q}$. Each d_q^h is a probability distribution over the finite state space \mathcal{S} , so it belongs to the probability simplex $\Delta^{|\mathcal{S}|-1}$. The full domain \mathcal{D}_{sv} is a Cartesian product of $K \times H$ such simplices. Each simplex is compact and convex, and thus their Cartesian product \mathcal{D}_{sv} is also compact and convex.

2. Frank-Wolfe Algorithm Steps:

Algorithm 2 implements the Frank-Wolfe algorithm:

- **Initialization (Line 13):** ${}^{(1)}d_{\text{mix},q} \leftarrow \mathbf{0}$. This initializes the iterate $D^{(1)}$ within \mathcal{D}_{sv} (the zero vector is on the boundary of the simplex if non-negativity is the only constraint, or can be seen as a valid (degenerate) visitation measure).
- **Gradient Computation (Line 16):** The algorithm computes the gradient $\nabla f(D^{(n)})$ (implicitly, by computing r_{grad_q} which is derived from this gradient).
- **Linear Maximization Oracle (LMO) (Lines 17-18):** For each q , the step $\pi_{\text{grad}_q}^{(n)} \leftarrow \text{value_iteration}(M, r_{\text{grad}_q})$ finds a policy that maximizes the linear objective $\sum_{s,a} d_\pi^h(s,a) r_{\text{grad}_q}(h,s,a)$ over all policies π . This is equivalent to finding a vertex $S_q^{(n)}$ of the polytope of visitation measures for policy q that maximizes $\langle \nabla_{d_q^h} f(D^{(n)}), S_q^{(n)} \rangle$. The collection of these $S_q^{(n)}$ for all q forms the $S^{(n)}$ in the standard Frank-Wolfe update $S^{(n)} = \arg \max_{S \in \mathcal{D}_{sv}} \langle \nabla f(D^{(n)}), S \rangle$. The computation of $d_{\text{grad}_q}^{(n)}$ from $\pi_{\text{grad}_q}^{(n)}$ yields this $S^{(n)}$.
- **Step Size (Line 20):** α_n is determined by exact line search: $\alpha_n \leftarrow \arg \max_{\alpha' \in [0,1]} f((1 - \alpha')D^{(n)} + \alpha' S^{(n)})$.
- **Update (Line 22):** $D^{(n+1)} \leftarrow (1 - \alpha_n)D^{(n)} + \alpha_n S^{(n)}$.

The algorithm performs $N_{iter} = N - 1$ such iterations, producing iterates $D^{(2)}, \dots, D^{(N)}$. (Note: $D^{(1)}$ is the initialization).

3. Convergence Rate: For a concave function f maximized over a compact convex set \mathcal{D} using the Frank-Wolfe algorithm with exact line search for the step size, the suboptimality gap $h_k = f(D^*) - f(D^{(k+1)})$ after k iterations (where $D^{(1)}$ is

the initial point and $D^{(k+1)}$ is the iterate after k Frank-Wolfe steps) is bounded by (Jaggi, 2013, Theorem 1 (Jaggi, 2013) and discussion for line search):

$$f(D^*) - f(D^{(k+1)}) \leq \frac{2C_f}{k+2}$$

where C_f is the curvature constant of f over \mathcal{D} , defined as

$$C_f = \sup_{\substack{X, S \in \mathcal{D}, \gamma \in (0, 1] \\ Y = (1-\gamma)X + \gamma S}} \frac{2}{\gamma^2} (f(X) + \gamma \langle \nabla f(X), S - X \rangle - f(Y)).$$

In our case, Algorithm 2 initializes with $D^{(1)}$ and performs N_{iter} iterations of the Frank-Wolfe update (corresponding to the loop variable n from 1 to N_{iter} in the algorithm’s notation as per Algorithm 2 where the loop runs $N - 1$ times; here we use N_{iter} to denote this count of iterations). The final iterate is $D^{(N_{iter}+1)}$. The standard bound $2C_f/(k+2)$ applies after k iterations. Here, $k = N_{iter}$. So, the suboptimality of the final iterate $D^{(N_{iter}+1)}$ is bounded by:

$$f(D^*) - f(D^{(N_{iter}+1)}) \leq \frac{2C_f}{N_{iter} + 2}$$

This holds for $N_{iter} \geq 1$. The constant C_f depends on the objective function f and the domain \mathcal{D}_{sv} . Since \mathcal{D}_{sv} is compact, C_f is well-defined and finite, provided f is continuously differentiable (which it is, assuming $s(\cdot)$ is, and $I_{total}(D)$ is differentiable).

Thus, Algorithm 2 converges to the global optimum with a rate of $O(1/N_{iter})$. \square

C. Vocabulary-Free Experimental Design via REINFORCE

We extend ED-PBRL to the vocabulary-free setting, where prompts are generated by learned LLM policies rather than selected from a fixed vocabulary. This enables optimization over the full space of natural language prompts, addressing scalability concerns about fixed vocabulary constraints.

C.1. Setup and Notation

We parameterize K prompt-generation policies using K copies of a pretrained GPT-2 model fine-tuned on Stable Diffusion prompts (MagicPrompt). Each policy $q \in [K]$ has learnable parameters θ_q and generates prompts autoregressively. In practice, policies share the same base initialization, and diversity is induced primarily through stochastic sampling (and optionally small initialization noise). All embeddings are computed using a *frozen* CLIP text encoder for computational efficiency; Stable Diffusion image generation occurs only after optimization, during feedback collection.

Truncated trajectory embeddings. Following the Truncated Trajectory Preference Feedback model (Section 3.4), we embed prompts at each word position, not just the final prompt. For a prompt $\tau_q = (w_1, w_2, \dots, w_H)$ from policy q consisting of H words, we use the truncated prefixes $\tau_q[1 : h] = (w_1, \dots, w_h)$ for $h = 1, \dots, H$, and embed each using the frozen CLIP text encoder:

$$\phi(\tau_q[1 : h]) = \text{CLIP}_{\text{text}}(\tau_q[1 : h]) \in \mathbb{R}^d \quad (15)$$

This gives $K \times H$ embeddings per trajectory (one per policy per word position), directly instantiating the per-timestep structure from the main ED-PBRL formulation. In our experiments, we use $H = 8$ words per prompt, yielding 32 embeddings per trajectory.

C.2. Per-Timestep Fisher Information

The Fisher Information structure directly instantiates the approximation from Section 4.3. Consider a single *trajectory*: a set of K prompts $\{\tau_1, \dots, \tau_K\}$, one sampled from each policy. At each word position $h \in [H]$, we have K truncated trajectory embeddings $\{\phi(\tau_q[1 : h])\}_{q=1}^K$.

Per-timestep contribution. The Fisher contribution at timestep h is:

$$I_h = \frac{1}{K} \sum_{q=1}^K \phi_q^{(h)} (\phi_q^{(h)})^\top - \mu_h \mu_h^\top \quad (16)$$

where $\phi_q^{(h)} := \phi(\tau_q[1:h])$ and $\mu_h = \frac{1}{K} \sum_{q=1}^K \phi_q^{(h)}$ is the mean embedding at timestep h . This is the empirical covariance of the K policy embeddings at position h .

Single-trajectory Fisher. The Fisher Information for one trajectory sums over timesteps:

$$I_{\text{traj}} = \sum_{h=1}^H I_h \quad (17)$$

This structure directly corresponds to Eq. (6) in the main paper, where the per-timestep visitation measures d_q^h are replaced by Monte Carlo samples from the learned policies.

C.3. Training Objective: Summing T Trajectories

A critical implementation detail is how multiple trajectories are combined. Let T denote the number of trajectories used to estimate the Fisher Information.

The training objective. We sample T independent trajectories and *sum* their Fisher contributions:

$$I = \sum_{t=1}^T I_{\text{traj}}^{(t)} + \lambda I_d = \sum_{t=1}^T \sum_{h=1}^H I_h^{(t)} + \lambda I_d \quad (18)$$

where $I_{\text{traj}}^{(t)}$ is the Fisher from trajectory t (Eq. 17), and $\lambda > 0$ is the regularization parameter. The D-optimal objective is:

$$\mathcal{L} = \log \det(I) \quad (19)$$

C.4. Monte Carlo Gradient Estimation

We use REINFORCE (the score function estimator) to optimize the non-differentiable sampling process. Let M denote the number of Monte Carlo samples used for gradient estimation.

Sampling structure. For each gradient step, we draw M independent *meta-samples*. Each meta-sample $m \in [M]$ consists of T trajectories, where each trajectory contains K prompts (one per policy). The total number of prompts generated per gradient step is $M \times T \times K$.

Per-sample objective. For meta-sample m , we compute:

$$I^{(m)} = \sum_{t=1}^T I_{\text{traj}}^{(m,t)} + \lambda I_d, \quad \mathcal{L}_m = \log \det(I^{(m)}) \quad (20)$$

Variance reduction via baseline. Raw REINFORCE has high variance. We use a *batch mean baseline*: the mean objective across the M samples within the current iteration:

$$\bar{\mathcal{L}} = \frac{1}{M} \sum_{m=1}^M \mathcal{L}_m \quad (21)$$

The centered advantage $(\mathcal{L}_m - \bar{\mathcal{L}})$ reduces variance while preserving the gradient's expected direction.

REINFORCE gradient. For policy q , the gradient estimate is:

$$\nabla_{\theta_q} \mathbb{E}[\mathcal{L}] \approx \frac{1}{M} \sum_{m=1}^M (\mathcal{L}_m - \bar{\mathcal{L}}) \cdot \nabla_{\theta_q} \log p_{\theta_q}(\mathcal{T}_q^{(m)}) \quad (22)$$

where $\mathcal{T}_q^{(m)}$ denotes all prompts generated by policy q in meta-sample m (i.e., T prompts), and:

$$\begin{aligned} \log p_{\theta_q}(\mathcal{T}_q^{(m)}) &= \sum_{t=1}^T \log p_{\theta_q}(\tau_q^{(m,t)}) \\ &= \sum_{t=1}^T \sum_{j=1}^{|\mathbf{z}_q^{(m,t)}|} \log p_{\theta_q}(z_j \mid z_{1:j-1}) \end{aligned}$$

Here $\mathbf{z}_q^{(m,t)}$ denotes the BPE token sequence of prompt $\tau_q^{(m,t)}$. In implementation, we accumulate token-level log-probabilities and use word boundaries only for constructing CLIP prefixes; the REINFORCE estimator uses the sum over token log-probabilities.

C.5. Algorithm

Algorithm 3 ED-PBRL with REINFORCE (Vocabulary-Free)

Require: K LLM policies with parameters $\{\theta_1, \dots, \theta_K\}$, frozen CLIP text encoder

Require: Hyperparameters: N (iterations), M (MC samples), T (trajectories per sample), H (words), λ (reg.), η (learning rate)

```

1: for  $n = 1, \dots, N$  do
2:   Sample: For each  $m \in [M]$ ,  $t \in [T]$ ,  $q \in [K]$ : sample prompt  $\tau_q^{(m,t)} \sim p_{\theta_q}$ 
3:   Embed: Compute  $\phi(\tau_q^{(m,t)}[1:h]) = \text{CLIP}_{\text{text}}(\tau_q^{(m,t)}[1:h])$  for all  $m, t, q, h \in [H]$ 
4:   for  $m = 1, \dots, M$  do
5:     for  $t = 1, \dots, T$  do
6:       for  $h = 1, \dots, H$  do
7:          $\mu_h^{(m,t)} \leftarrow \frac{1}{K} \sum_{q=1}^K \phi(\tau_q^{(m,t)}[1:h])$ 
8:          $I_h^{(m,t)} \leftarrow \frac{1}{K} \sum_{q=1}^K \phi(\tau_q^{(m,t)}[1:h]) \phi(\tau_q^{(m,t)}[1:h])^\top - \mu_h^{(m,t)} (\mu_h^{(m,t)})^\top$ 
9:       end for
10:      end for
11:       $I^{(m)} \leftarrow \sum_{t=1}^T \sum_{h=1}^H I_h^{(m,t)} + \lambda I_d$  {Sum  $T$  trajectories, Eq. 18}
12:       $\mathcal{L}_m \leftarrow \log \det(I^{(m)})$ 
13:    end for
14:     $\bar{\mathcal{L}} \leftarrow \frac{1}{M} \sum_{m=1}^M \mathcal{L}_m$  {Batch mean baseline}
15:    for  $q = 1, \dots, K$  do
16:       $g_q \leftarrow \frac{1}{M} \sum_{m=1}^M (\mathcal{L}_m - \bar{\mathcal{L}}) \cdot \nabla_{\theta_q} \log p_{\theta_q}(\mathcal{T}_q^{(m)})$  {Eq. 22}
17:       $\theta_q \leftarrow \theta_q + \eta \cdot g_q$  {Gradient ascent}
18:    end for
19:  end for
20: Return: Optimized policies  $\{p_{\theta_q}\}_{q=1}^K$ 

```

After optimization, prompts are sampled from the learned policies and passed to Stable Diffusion for image generation. Preference feedback is then collected and used to estimate $\hat{\theta}$ as in the standard ED-PBRL pipeline.

C.6. Direct Optimization of Truncated Trajectory Fisher

A notable advantage of the REINFORCE formulation is that it directly optimizes the Fisher Information for the *truncated trajectory* feedback model (Section 3.4). In the main Frank-Wolfe approach, tractability requires optimizing the state-based Fisher, which only indirectly improves the truncated trajectory Fisher via Theorem 4.2 (under an additive feature assumption). The REINFORCE approach bypasses this indirection: since we compute embeddings $\phi(\tau[1:h])$ of actual truncated prompts, the Monte Carlo Fisher estimate (Eq. 18) directly targets the quantity we care about. The trade-off is a non-convex optimization landscape, but our experiments show that REINFORCE with variance reduction still achieves consistent improvement.

Practical hyperparameters. We run $N = 200$ optimization iterations with $M = 8$ Monte Carlo samples for gradient estimation, $T = 8$ trajectories per sample for Fisher estimation, and $H = 8$ words per prompt. We use $\lambda = 1$ regularization and learning rate $\eta = 10^{-3}$ with SGD. The baseline model is MagicPrompt (GPT-2 fine-tuned on 80k Lexica.art prompts for Stable Diffusion). All $K = 4$ policies are updated jointly at each iteration. See Table 2 for the complete parameter summary.

C.7. Additional Experimental Details

The main experimental results for the REINFORCE extension (optimization trajectory and t-SNE visualization) are presented in Figure 5 in Section 6.3. Here we provide an additional quantitative metric for embedding space structure.

Between-policy cosine similarity. To quantitatively assess whether the $K = 4$ optimized policies learn complementary prompt distributions, we analyze the pairwise similarity of their CLIP embeddings. We sample 10 prompts from each policy, repeat this for 10 independent draws, and compute the mean cosine similarity between prompts from *different* policies (lower indicates more diversity). Figure 15 reports the mean \pm std across repeats. ED-PBRL yields substantially lower between-policy similarity (0.140 ± 0.006) than the unoptimized MagicPrompt baseline (0.185 ± 0.012), indicating more structured diversity in the learned prompt generators; the low standard deviation across repeats suggests this effect is stable.

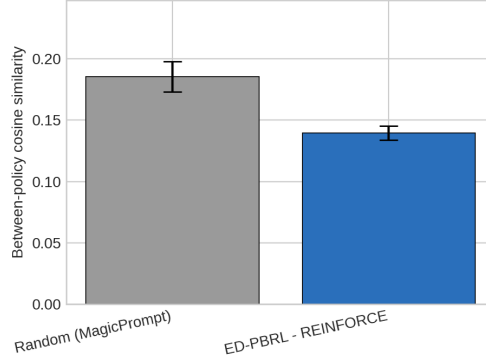


Figure 15. Between-policy cosine similarity of CLIP embeddings (mean \pm std across 10 repeats; 10 prompts per policy). Lower values indicate more diverse policies. ED-PBRL achieves 24% lower similarity than the random baseline.